Deterministic mapping of potential landslide debris inundation in the Kaikōura District

MA Brideau
B Lukovic
CI Massey
R Morgenstern

GNS Science Consultancy Report 2019/102
March 2020

DISCLAIMER

This report has been prepared by the Institute of Geological and Nuclear Sciences Limited (GNS Science) exclusively for and under contract to Canterbury Regional Council. This report considers landslide hazards. As there is always uncertainty inherent within the nature of natural events, GNS Science gives no warranties of any kind concerning its assessment and estimates, including accuracy, completeness, timeliness or fitness for purpose. Unless otherwise agreed in writing by GNS Science, GNS Science accepts no responsibility for any use of or reliance on any contents of this report by any person other than Canterbury Regional Council and shall not be liable to any person other than Canterbury Regional Council, on any ground, for any loss, damage or expense arising from such use or reliance.

Use of Data:

Date that GNS Science can use associated data: February 2020

BIBLIOGRAPHIC REFERENCE

Brideau MA, Massey CI, Lukovic B, Morgenstern R. 2020. Deterministic mapping of potential landslide debris inundation in the Kaikōura District. Lower Hutt (NZ): GNS Science. 37 p. Consultancy Report 2019/102.

CONTENTS

FIGURES

TABLES

EXECUTIVE SUMMARY

Canterbury Regional Council (CRC) and the Kaikōura District Council (KDC) commissioned the Institute of Geological and Nuclear Science (GNS Science) to map areas of the KDC district that could potentially be affected by landslides triggered by earthquakes and/or rainfall. It is our understanding that the results from this project may be used to underpin parts of the KDC District Plan change with regards to their natural hazards chapter, which is being reviewed after the M_W7.8 14 November 2016 Kaikōura earthquake.

This project focuses on landslides that include both “slippage” and “falling debris” hazards, terms mentioned in the Building Act (2004), and used in this report as:

1. Slippage includes the movement or loss (including partial loss) of land from a slope when it occurs beneath a structure (e.g., dwelling, garage, road, shed, etc.), and;
2. Falling debris includes soil, rock, vegetation, snow or ice that may fall and “runout” onto a property (e.g., dwelling, garage, shed and/or land), from upslope (the landslide source area), inundating the property.

The work presented in this report comprises a district-scale assessment of selected landslide hazards (debris and rock avalanches and debris flows) within the project area. The project objectives were:

1. To provide a district-scale deterministic assessment of locations within the project area that could be affected by debris and rock avalanches (slippage and falling debris hazards) triggered by earthquakes and rain; and
2. Delineate the location and extent of debris-flow fans within the project area and provide a district-scale deterministic assessment of potential debris inundation areas from debris flows triggered by rainfall.

This Phase 1 report summarises the methodology used to provide a district-scale deterministic assessment of the locations within the project area that could be affected by debris and rock avalanches (slippage and falling debris) and debris flows (debris-flow fans) triggered by earthquakes and rain. The landslide debris inundation areas were modelled in ArcGIS using a set of empirical relationships based on observations of landslides in New Zealand and worldwide. The landslide debris inundation modelling was carried out for three landslide types: 1) debris flows; 2) debris avalanches; and 3) rock avalanches. This report provides example applications of the methodology used. The ArcGIS data files of the results for the entire project area are provided to CRC and KDC.

Results from this project highlight that rainfall-triggered landslides (wet debris avalanches and debris flows) have a greater mobility and travel further than earthquake-triggered landslides (dry debris avalanches) of similar volume. These results are consistent with research by others in New Zealand and worldwide. This project also provides information which could be used to delineate areas with greater potential for landslide debris inundation (i.e. located downslope from potential landslide sources and within modelled runout distances based on empirical relationships). Due to the deterministic nature of the assessment presented in this report, it does not provide a probability of occurrence for the landslide hazard scenarios considered. This means that while estimates of landslide debris inundation are available for a range of landslide types and volumes, the current Phase 1 work does not provide information regarding the likelihood of a given area being inundated with debris.

It is recommended that KDC and CRC assess whether the results from this Phase 1 study provide sufficient information to underpin District Plan provisions. The Phase 2 work would take the results from Phase 1 and estimate the spatial probability of landslides of different volumes impacting the different areas within the hazard zones identified in Phase 1. Whilst we understand that this Phase 2 work may not be needed, it would provide a more robust analysis of the landslide hazards within the district.

This page left intentionally blank.

1.0 INTRODUCTION

Canterbury Regional Council (CRC) and the Kaikōura District Council (KDC) commissioned the Institute of Geological and Nuclear Science (GNS Science) to map areas of the KDC district that could potentially be affected by landslides triggered by earthquakes and/or rainfall. It is our understanding that the results from this project may be used to underpin parts of the KDC District Plan change with regards to their natural hazards provisions, which is being reviewed after the M_W7.8 14 November 2016 Kaikōura earthquake.

The scope-of-work, extent of project area, and budget were outlined in GNS Science proposal 24766267, which was approved by CRC on 21 June 2019. This project is conducted under the terms of the Master Service Agreement (MSA) 1121-20/21 between GNS Science and CRC for the period May 2018 to April 2021. The area covered in this project is shown in Figure 1.1.

It was proposed by GNS Science, that this work be carried out in two phases:

- Phase 1: To provide a district-scale deterministic assessment of the locations within the project area that could be affected by landslide hazards; and
- Phase 2: To provide a district-scale probabilistic assessment of the landslide hazards identified in Phase 1.

Phase 2 cannot be carried out without completing Phase 1. However, the Council may not need to carry out Phase 2, if the results from Phase 1 provide the information they need to underpin parts of the KDC District Plan change. This report provides the results from Phase 1.

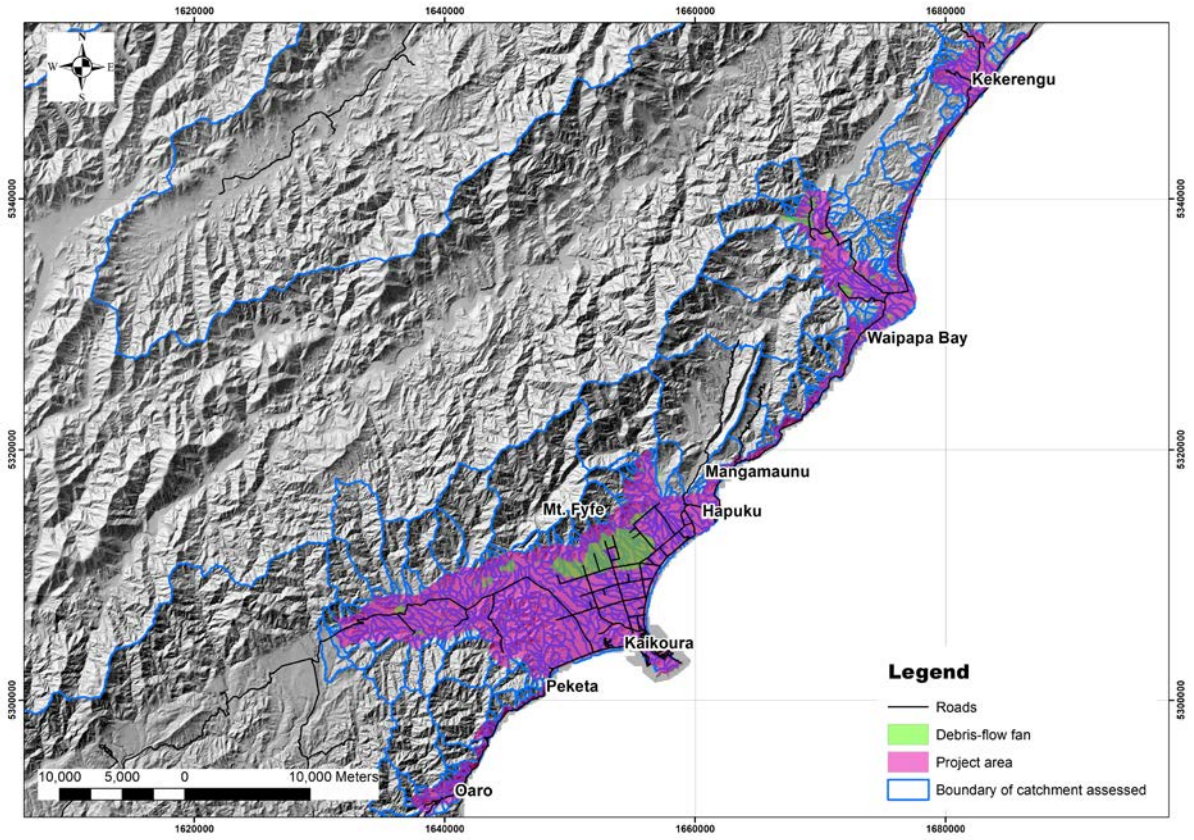

Figure 1.1 Overview map of the project area.

1.1 Terminology

The Resource Management Act (1991) defines natural hazards as “any atmospheric or earth or water related occurrence (including earthquake, tsunami, erosion, volcanic and geothermal activity, landslip, subsidence, sedimentation, wind, drought, fire, or flooding) the action of which adversely affects or may adversely affect human life, property, or other aspects of the environment”. This project focuses on landslides that include both “slippage” and “falling debris” hazards (Figure 1.2), as mentioned in the Building Act (2004), and used in this report as:

1. Slippage includes the movement or loss (including partial loss) of land from a slope when it occurs beneath a structure (e.g., dwelling, garage, road, shed), and;
2. Falling debris includes soil, rock, vegetation, snow or ice that may fall and “runout” onto a property (e.g., dwelling, garage, shed and/or land), from upslope (the landslide source area), inundating the property.

Slippage might include extremely rapid (5 m/s) to extremely slow (< 16 mm/year) debris movement velocity, but falling debris tends to involve extremely rapid (5 m/s), and very rapid (3 m/min) debris movement velocity, e.g., rockfall and debris flows.

For this report the term landslide debris inundation area refers to the runout path that is inundated by the debris which includes the debris source, transport, and deposit zones (Figure 1.3).

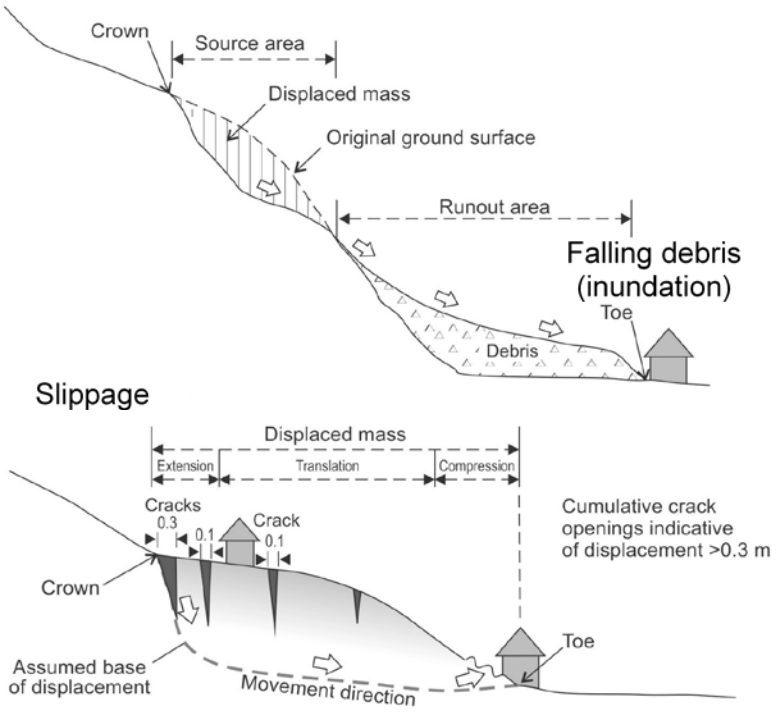

Figure 1.2 Schematic diagrams by GNS Science showing landslide hazards in terms of “falling debris” and “slippage” used in the Building Act (2004).

The Earthquake Commission (EQC) Act (1993) refers to landslides as: “natural landslip meaning the movement (whether by way of falling, sliding, or flowing, or by a combination thereof) of ground-forming materials composed of natural rock, soil, artificial fill, or a combination of such materials, which, before movement, formed an integral part of the ground;

but does not include the movement of ground due to below-ground subsidence, soil expansion, soil shrinkage, soil compaction, or erosion".

Landslides are defined as the movement of rock, soil, or debris downslope (Evans 2001). According to the velocity scale proposed by Hungr et al. (2014), landslides can range from extremely rapid (> 5 m/s) to extremely slow (< 16 mm/year). Skempton and Hutchinson (1969) noted that the landslide deformation history comprises three distinct episodes: pre-failure deformation; the failure itself; and post-failure displacement. Many landslides exhibit several movement episodes, separated by long or short periods of relative quiescence. Landslides are typically categorised following the scheme of Hungr et al. (2014), which describes their type of movement and the material in which they originate.

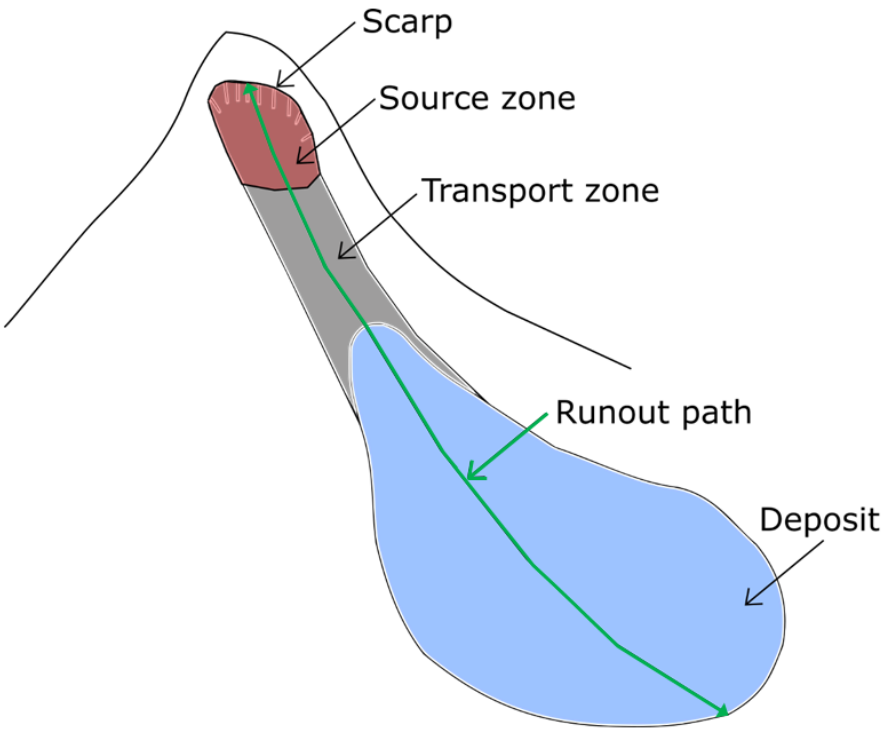

Figure 1.3 Schematic representation of the source area and debris inundation area (source, transport, and deposit zones) of a landslide. Drawing modified from Mitchell et al. (in press).

1.2 Objectives

It is important to note that this work comprises a district-scale assessment of selected landslide hazards within the project area. The project objectives are:

1. To provide a district-scale deterministic assessment of locations within the project area that could be affected by slippage and falling debris triggered by earthquakes and rain.
2. Delineate the location and extent of debris-flow fans within the project area and provide a district-scale deterministic assessment of potential debris inundation areas from debris flows triggered by rainfall.

1.3 Landslide Types Assessed and Associated Definitions

Understanding what landslide type can occur at a given location is important since the different landslide types have typical behaviour (e.g., velocity of displacement, reoccurrence, travel distance) which affects how hazardous they can be. Based on the classification by Hungr et al. (2014), the rapidly moving landslide types assessed in this project are: 1) debris flows; 2) debris avalanches; and 3) rock avalanches. These three types of landslides cover both slippage and falling debris as defined in the Building Act (2004). Inundation by slow moving landslides has not been assessed as part of this project.

1.3.1 Debris Flows

Debris flows are defined by Hungr et al. (2014) as a "very rapid to extremely rapid surging flow of saturated debris in a steep channel. Strong entrainment of material and water from the flow path can occur along the runout path. Debris flows often occur simultaneously with floods. The debris flow may be initiated by a debris slide, debris avalanche or rockfall from a steep bank, or by spontaneous instability of the steep stream bed." The sediment concentration of debris flows exceeds 40% (typically 50–70%) and their volume can be up to 1,000,000,000 m^3 (Iverson et al. 2011). Figure 1.4 shows the result of a mobile channelised debris flow.

Once saturated debris material begins to move in a steep channel, the volume of a debris flow can change due to entrainment (Iverson et al. 2011). Entrainment results from scour of channel bed sediment or collapse of stream banks. The bulk of the material involved in a debris-flow event can sometimes originate from entrainment within the runout path. Experimental results from Iverson et al. (2011) have shown that pore water pressures generated as wet bed sediment is overridden and progressively entrained by debris flows can reduce friction and lead to a pronounced increase in flow-momentum. The pore water pressure represents the pressure exerted by the water filling the voids in a soil, debris, or rock mass. Changes in debris-flow volume and momentum due to entrainment have the potential to influence the debris-flow velocity and travel distance (Iverson et al. 2011).

Following Hungr et al. (2014), a debris flow refers exclusively to a channelised landslide, whereas a landslide consisting of flowing debris on an open slope is referred to as a debris avalanche. It is possible that debris flows become debris avalanches (Section 1.3.2) if the channel they flow down becomes less confined, and conversely debris avalanche may become debris flows if the debris enters a channel. Where the erosion rate outpaces the depositional environment (e.g., river or coastal erosion rate greater than deposition rate), the landslide deposits from multiple debris flows form debris fans. Wilford et al. (2004) noted that fans constructed by debris flows "characteristically have marginal levees or terminal lobes."

Figure 1.4 Debris flows triggered by rain in Eastbourne, Wellington, in November 2006. The source areas of the debris flows are in the left of the photograph. The debris travelled down slope several hundreds of meters where it impacted the dwellings shown in the right of the photograph. Photograph by G. Hancox, GNS Science.

1.3.1.1 Fan

Fans are cone-shaped landforms that are generated when confined watercourses (e.g., gullies, creeks, rivers) become wider and the water course becomes less confined, e.g., when watercourses enter valleys, plains or lakes. The resulting decrease in flow velocity promotes sediment deposition. Mapping the extent of fans is important because they are dynamic landforms that result from cyclic avulsion of channels radiating from the fan apex (Figure 1.5). The dynamic nature of such landforms poses a hazard to people and infrastructure located on them; as areas that were inactive (and have since been built on) can reactivate and start actively eroding or receiving sediments. Davies and McSaveney (2008) discussed some of the considerations for sustainable development on fans. Davies and McSaveney (2008) also discussed that fans can be divided into two end-members: 1) alluvial fan – dominated by deposition of sediment from fluvial processes; and 2) debris-flow fan – dominated by deposition of sediment from debris flows and debris floods (Figure 1.6). This report focuses on delineating the extent of both types of fans and identifying the likely dominant fan-building process. As debris-flow fans are typically associated with comparatively small and steep catchments, morphometric (i.e., measurements of the landscape shape) parameters such as the Melton Ratio (defined in Section 1.3.1.2) can be used to estimate the dominant fan-building process (fluvial vs. debris flow).

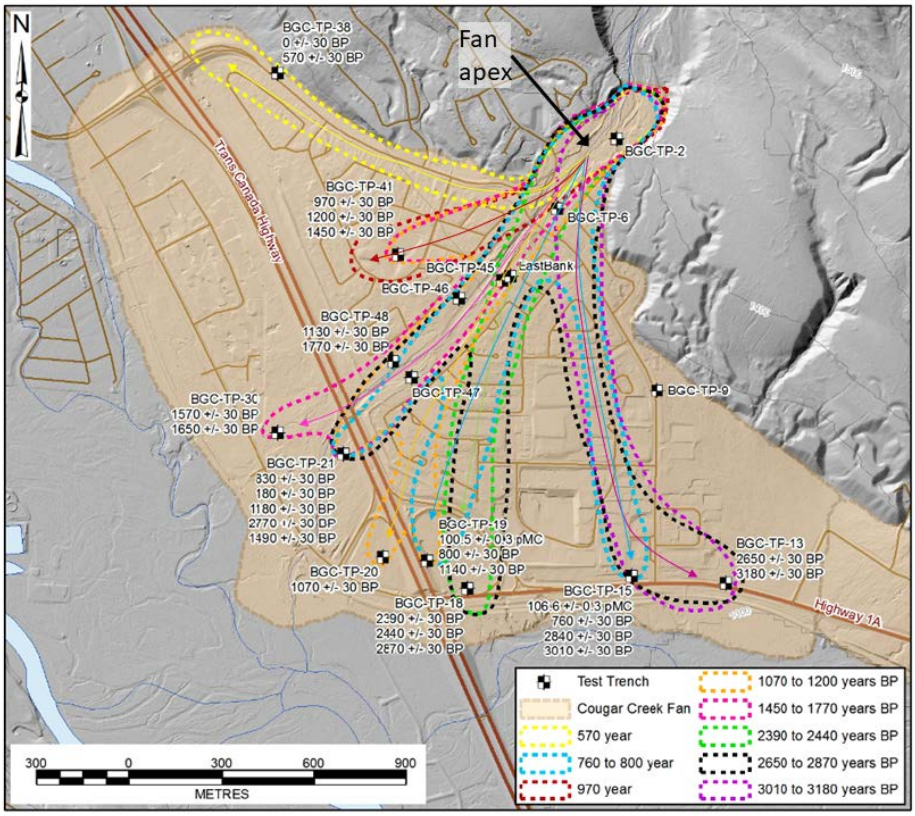

Figure 1.5 Example from Cougar Creek, Alberta, Canada of the different sections of a fan receiving sediment during the last ~3,200 years (modified from Jakob et al., 2017).

Figure 1.6 Oblique aerial view of debris-flow fans in the Makarora valley. Photograph by L. Homer, 1996 GNS Science.

1.3.1.2 Melton Ratio

The Melton Ratio was first defined by Melton (1965) as the topographic relief of the catchment ($\Delta H_{catchment}$ which is highest elevation minus lowest elevation in the catchment) divided by the square root of its area ($A_{catchment}$).

$$Melton\ Ratio = \frac{\Delta H_{catchment}}{\sqrt{A_{catchment}}}$$

The Melton Ratio has been used to identify debris-flow dominated catchments in New Zealand, for example, in the Southern Alps (de Scally and Owen 2004; Kritikos and Davies 2015), the Coromandel and the Kaimai ranges (Welsh 2007), along with the Bay of Plenty and Westland (Welsh and Davies 2011) regions.

1.3.1.3 Debris Floods

A debris flood is defined by Hungr et al. (2014) as a landslide consisting of "very rapid flow of water, heavily charged with debris, in a steep channel, whose peak discharge is comparable to that of a water flood". Pierson (2005) referred to them as hyper concentrated flows that are transitional between debris flows and water floods. In the current project, debris floods are distinguished from debris flows, using the Melton Ratio and catchment length assessment to determine the dominant fan forming process.

1.3.2 Debris Avalanches

A debris avalanche is defined by Hungr et al. (2014) as a "very rapid to extremely rapid shallow flow of partially or fully saturated debris on a steep slope, without confinement in an established channel". In the project area, the term debris avalanche was restricted to landslides with a volume less than 100,000 m^3 (above which landslides were considered to be a rock avalanche, Section 1.3.3). Hungr et al. (2014) also described debris avalanches as initiating as debris slides (Section 1.3.2.1) and are associated with failures of residual soil, colluvial, pyroclastic, or organic veneer.

The important distinction between debris avalanches and rockfalls is that rockfalls comprise individual fragments, which move as independent rigid bodies interacting with the substrate by means of episodic impacts. By contrast, debris avalanches move in a flow-like manner as masses of interacting fragments and water. Figure 1.7 provides examples of debris avalanches from the Kaikōura District.

Figure 1.7 Debris avalanches triggered by the 2016 Kaikōura earthquake. Photograph by D. Townsend, GNS Science.

1.3.2.1 Debris Slides

A debris slide is defined by Hungr et al. (2014) as a: “sliding of a mass of granular material on a shallow, planar surface parallel with the ground. Usually, the sliding mass is a veneer of colluvium, weathered soil, or pyroclastic deposits sliding over a stronger substrate. Many debris slides become flow-like after moving a short distance and transform into extremely rapid debris avalanches.” Debris slides are not analysed separately in this project and this definition is only provided to describe the initial stage of a debris avalanche (Section 1.3.2).

1.3.3 Rock Avalanches

A rock avalanche is defined by Hungr et al. (2014) as: “an extremely rapid (> 5 m/s), massive, flowlike motion of fragmented rock from a large rock slide or rock fall. Large rock avalanches have a degree of mobility that exceeds the behaviour of a smaller-volume frictional flow of dry, angular, broken rock.” The mobility of rock avalanches, which affects the runout distance, increases systematically with the volume of the event. To capture the increase of mobility as a function of volume, the current project restricted the use of rock avalanches to landslides having a volume greater than 100,000 m^3. Figure 1.8 provides examples of a rock avalanche from the Kaikōura District.

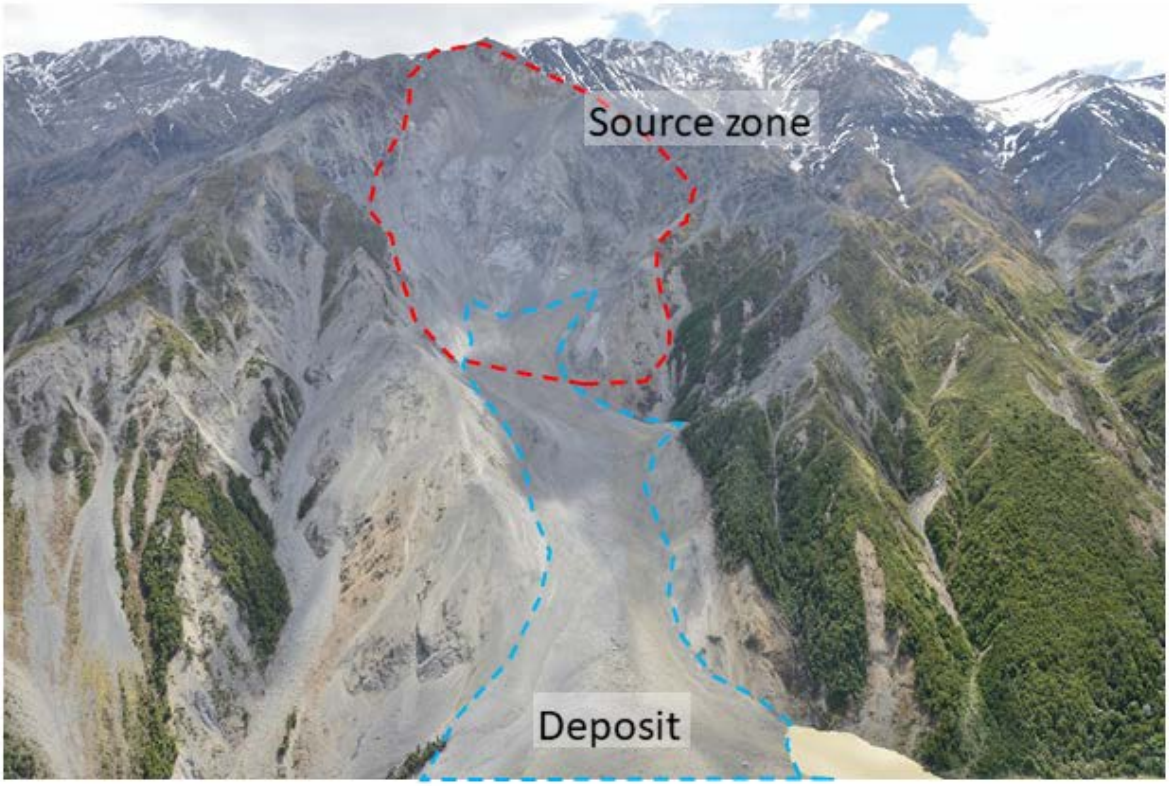

Figure 1.8 Hapuku rock avalanche triggered by the 2016 Kaikōura earthquake. The deposit extends outside current field-of-view. Photograph by D. Townsend, GNS Science.

1.4 Exclusions

For those landslide types assessed, the results from this project do not provide an estimate of the depth or velocity of the debris as it reaches the inundation area delineated in the maps.

The results from this project exclude debris inundation from rockfalls (i.e., the fall of single or a few rock blocks). It excludes ground movement by slow moving landslides such as rotational sliding (slumps), earthflows, and deep-seated gravitational slope deformation (DSGSD). While DSGSD landslide types represent a lower life safety hazard – as they tend to move slowly – they can still result in significant infrastructure damage (e.g., Mansour et al. 2011). Slow moving landslides can, under certain conditions, evolve into or be associated with rapid landslides (e.g., Reid et al. 2003; Loew et al. 2017) in which case if they meet the topographic criteria defined in Section 2.5.2.1 they will be covered by the analyses conducted in this project. What is not covered by this project, is the slow displacement component of such landslides.

The results from this project exclude inundation from water, sediment and/or debris (at concentrations lower then debris flows) resulting from fluvial flooding (flash flood or freshet). Fluvial flooding hazard in the Kaikōura Regional District is discussed in Wild (2020). Debris inundation from a landslide dam breach is also not included as it would require estimates of the valley blocking potential, landslide dam volume, time to failure of the dam after the landslide, and dam failure mechanism (rapid or progressive failure).

Entrainment along the travel path was not explicitly modelled in this project as the landslide volume was assumed to be constant from the start to end points. Multiple landslide volumes, however, were considered in each analysis based on topographic criteria (Section 2.5.2.1).

The results of this project do not provide a likelihood (probability) of a landslide occurring on a given slope, or likelihood of debris reaching a given location within the inundation area. These likelihoods could be estimated in a follow-up stage to the work presented in this report.

1.5 Limitations

The landslide debris inundation extents reported in this project are estimated based on the 50% runout exceedance extent for a landslide type of a given volume (Section 2.5.1). This implies that in 50% of the cases it can be anticipated that the landslide debris would extend further than reported and in 50% of cases it can be anticipated that the landslide debris would extend less than reported. A probabilistic approach which considers the likelihood estimate of the occurrence of the different landslide volumes for each landslide type along with cumulative likelihood estimates of debris inundation from these various landslide scenarios could be undertaken to further characterise the landslide debris inundation hazard.

The results from this project provide a district-scale deterministic assessment of the landslide-debris inundation potential. It is of adequate scale and detail to identify general areas susceptible to slippage and/or landslide-debris inundation. It should not be used to inform site-specific determinations or the design of landslide mitigation measures, which would require a sufficiently detailed and rigorous site-specific landslide assessment carried out by a qualified practitioner.

2.0 METHODOLOGY

This section provides an overview of the different steps and techniques used to: 1) identify and define the extents of the debris-flow fans; 2) calculate the Melton Ratios; and 3) derive the theoretical background for empirical-relationships for estimating the landslide debris inundation zones and their implementation in the Geographical Information System (GIS) environment. The methodology outlined below follows, where appropriate, the guidelines for landslide susceptibility zoning outlined in Fell et al (2008).

2.1 Delineation of Fans

Fan delineation was conducted in ArcGIS using:

1. Hillshade and slope angle models along with one metre topographic contours, all derived from the 2016 LiDAR, captured after the M_W 7.8 14 November 2016 Kaikōura earthquake;
2. Post-earthquake aerial ortho-imagery from 2016 and 2019, which show the effects of the Kaikōura earthquake and the ex-tropical cyclones Debbie (4–6 April 2017), Cook (13–14 April 2017), and Gita (20 February 2018); and
3. Historical aerial photographs from 1975 and 1976, which show the effects of cyclone Allison (11–12 March 1975), which are available on retrolens.nz.

Fans were delineated where the topographic contours showed a reversal of curvature – defined by a concave break in slope – where the watercourse (channel) changes from being confined to less-confined (Figure 2.1). The fan apex was chosen to represent the location where the gully, creek, stream or river became less-confined (Figure 2.1).

The fan extents were mapped using the current morphology as shown by the post-Kaikōura earthquake 2016 LiDAR survey, which was used as the basis for the mapping. However, the mapped fan boundaries should be considered as transitional as they are likely to change in the future as more material is deposited on them or eroded from them. Therefore, sediment deposition is possible beyond the currently mapped fan limits. Floods, debris floods, and debris flows could travel further than the currently mapped fan extent, as the fans may have been modified by anthropogenic (e.g., road) and natural (river erosion) processes or due to an extreme landslide event. The minimum fan area considered was 500 m^2, as it was the smallest size that could confidently and systematically be mapped in the project area based on the available information. A 500 m^2 fan also represents the assumed smallest size on which a building as defined in the Building Act (2004) is likely to be located. One fan smaller than 500 m^2 was included, as its current extent is truncated by State Highway 1 (i.e., its likely natural extent would be greater) and it is located at the base of a well-defined gully channel.

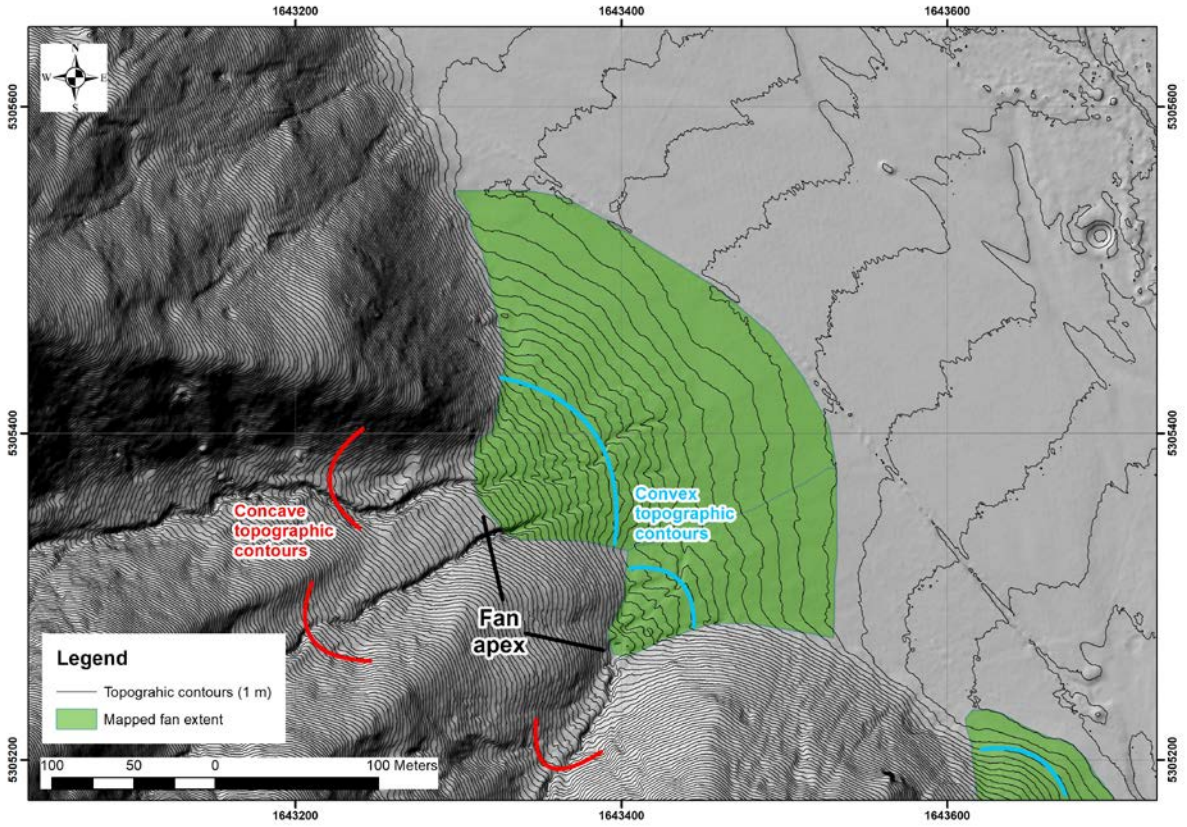

Figure 2.1 Example of fan delineation in the project area based on topographic contours.

2.2 Stream Order

A commonly used classification to characterise the hydrology and ecology of a stream is the stream order. Stream order was used in this project to quantify the stream size and complexity and provide a cut-off for which fans were mapped. Larger stream orders typically indicate larger catchments with a lower overall channel gradient, which lead to fluvial processes dominating the resulting fan.

Based on the classification system outlined in the River Environment Classification (REC) by the Ministry for the Environment (MfE, 2010), a stream order represents the numerical position of a tributary within a catchment. When two tributaries of the same stream order join, the segment downstream of their confluence is given a higher stream order (Figure 2.2). Initially, the catchment area from the REC (MfE 2010) was used to calculate the Melton Ratio. The REC uses a 30 m grid resolution to define the catchment boundaries. A preliminary assessment of the fan delineation and catchment boundaries found the spatial resolution of the REC catchments to be too coarse relative to the scale of fan mapping. New delineation of catchments was therefore undertaken for this project using the national 8 m Digital Elevation Model (DEM) grid available for New Zealand (LINZ 2012). The 2016 LiDAR (1 m grid resolution) was not used to define the catchments as it does not cover the headwaters of all of the catchments included in the project area, particularly those with larger stream orders of 5 and 6.

Numerous researchers (e.g. Bigelow et al. 2007) noted that debris flows typically initiate in first- and second-order streams. As debris inundation occurs downstream of the initiation point, fan extent was delineated in this project for catchments drained by streams of order 3 or lower.

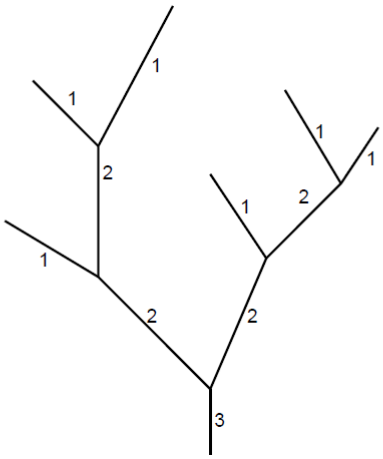

Figure 2.2 Schematic representation of how the order of a stream is defined in the River Environment Classification (REC) by the Ministry for the Environment (MfE 2010). This is the stream order definition used in this project.

2.3 Catchment Morphometry

In this project, catchment morphometry (i.e., measurement of landscape shape) is used to estimate the dominant hazard in a catchment. Wilford et al (2004) conducted a study in west central British Columbia, Canada, which investigated what morphometric parameters are the most useful to estimate which hazard (flood, debris flood, debris flow) is the dominant one within a given catchment. They found that the "Melton Ratio" and the catchment length were the best indicators of the dominant process/hazard.

In this project we use the Melton Ratio and catchment length to classify each of the mapped fans based on their dominant hazard type (Table 2.1). We also use the optical imagery and fan morphology to check whether debris-flow deposits (lobate-shaped deposits of mixed fine- to coarse-grained debris) could be identified. Dominant hazard type based on Table 2.1 was also compared with field observations of fan morphology and debris characteristics during field verification (Section 2.6). It should be emphasised that using the Melton Ratio and catchment length for estimating the dominant hazard is an empirical approach and that hazards other than the dominant one are also possible on a fan, based on site-specific and meteorological event-specific conditions. For example, Welsh and Davies (2011) noted that in two cases from their study, fans with documented debris-flow activity (Awatarariki and Waiteperu) were not identified as such based on the criteria outlined in Table 2.1.

Table 2.1 Summary of the Melton Ratio and catchment length used to estimate the dominant hazard type at each fan.

Dominant hazard type	Melton Ratio	Catchment length (km)
Flood	< 0.3	-
Debris flood	0.3–0.5	> 2.7
Debris flow	> 0.5	< 2.7

2.3.2 Catchment Morphometry in ArcGIS

The following methodology was used to define the catchment boundaries and calculate their Melton Ratios and catchment lengths:

1. The 8 m DEM was 'filled' using the Fill tool to remove artificial 'sinks' or depressions – the assumption was made that all sinks are artefacts. It is important to remove these artificial depressions as they have the potential to influence the modelled flow of streams and rivers.
2. The Flow Direction and Flow Accumulation grids were created to establish the flow path of streams and rivers.
3. A 'pour point' – defined as a point on the surface where water exits the catchment (ESRI 2018) – was then placed for each catchment within each stream order (orders 1 to 6 – using the stream orders assigned by REC where applicable). For this project, pour points were placed manually on the apex of the mapped fans. Each of these pour points was assigned a unique identifier that could be matched to its corresponding catchment. Although each point had to be placed within the pixel corresponding to the highest flow accumulation, the Snap Pour Points tool ensures the right pixel has been selected (a search distance of 8 m was used, corresponding to the resolution of the DEM).
4. Catchments (classified by stream order) were firstly defined based on the Snapped Pour Point and Flow Direction grids. In some cases, this was an iterative process, as catchment delineation occurs only after pour points have been placed, and placement will affect subsequent calculation of the Melton Ratio.
5. Zonal Statistics were calculated (in ArcGIS) for each catchment using the 'filled' 8 m DEM to generate values for maximum elevation, minimum elevation, and area. From those, it was possible to calculate relief, square root of the area, and the Melton Ratio.
6. The length of catchments was estimated using grid analysis within ArcGIS. The stream network within each catchment was delineated from the DEM using the output from the Flow Accumulation tool. The stream network grid, with a value of 1 in each cell identifying a stream, was then used as an input to the Cost Distance tool which calculated the cumulative distance between the pour point and each cell within the stream network. The maximum value in the resulting distance grid was assumed to be associated with the cell furthest from the pour point and provided an estimate of the catchment length.

2.5 Landslide Debris Inundation

The distance that landslide debris travels down a slope from a potential source area is usually referred to as the landslide travel distance or runout distance (e.g., McDougall 2017). Under certain conditions some landslides can also travel a certain distance up the opposite side of the valley (e.g., Evans et al. 1994). The debris inundation area is defined as the area of ground that falling debris may cover as it travels, which comprises the source zone, transport zone, and the deposition zone (Figure 1.3). Numerous techniques exist to estimate the potential landslide debris runout and inundation area. These typically fall into two categories: 1) empirical; or 2) physics-based methods. Empirically-based methods rely on the debris inundation area of past landslides of a given type, to estimate the anticipated debris inundation area of future landslides of a similar type. They are relatively simple to apply which makes them appropriate for district-scale studies. Because empirically-based methods record the actual behaviour of landslides, they are not limited by our current understanding of landslide mechanics as can be the case in physics-based models. A limitation of the empirically-based debris inundation model used in this project is that is cannot incorporate the site-specific conditions in the forward-looking estimates of the debris inundation area.

Physics-based methods include a range of techniques that consider the site-specific topography (usually in 2D or 3D) landslide volume, and equivalent rheological parameters of the failed landslide mass (e.g., Hungr and McDougall 2009; Christen et al. 2012). Such techniques need to be calibrated by back analysing a suite of data from representative landslides of varying types, from which detailed information about the landslide can be obtained and used in the calibration. Iverson (2014) noted that because there is often not enough information available to fully constrain a physics-based debris-flow model, empirical methods (i.e., back analyses of historical events) continue to play a dominant role in estimating the hazard associated with debris flows.

Using such physics-based approaches for the current district-scale assessment is not possible, as they take considerable input data and time to set up, calibrate, and run, and as such, we have adopted the empirically-based methodology.

2.5.1 Empirical Relationship

Heim (1932) proposed that the distance a landslide travels is proportional to its fall height. The tangent of the ratio of the fall height (ΔH) to horizontal runout distance (L) between the crest of the source zone and toe of the deposit, known as the “Fahrböschung” (Figure 2.3), has subsequently been correlated with landslide volume (V) (Figure 2.3). Empirical relationships between the Fahrböschung and landslide volume have been derived for different landslide types (e.g., Corominas 1996). In this project, the landslide trigger (earthquake or rain) was used as a proxy for the initial water content of the landslide source material. All other factors being equal, source material with higher water content (i.e., rain triggered) typically results in longer runout distance. Measurement of the slope crest and deposit toe can be compiled for many different landslide types and trigger conditions to generate empirical relationships similar to the one in Figure 2.3. From these compilations, a best fit linear regression (in log-log space) between ΔH/L and V was derived for each landslide type (debris avalanche, rock avalanche, and debris flow) and trigger (seismic/dry and rainfall/wet).

Empirically-based relationships between ΔH/L and V represent the compilation of landslides with different site conditions (e.g., source geology, local topography, grain-size of failed material, water content of source material and erodible material along travel path, vegetation, buildings, the presence (or not) of mitigation measures). This range of site-specific conditions

results in the variability of observed landslide debris runout and inundation area. The variability in the landslide debris runout and inundation data also allows for the probability of runout exceedance, or limits of confidence to be defined for the prediction of runout for each landslide volume (e.g., Li 1983). For example, the best fit (orange) line in Figure 2.4, represents an exceedance probability of 50%, i.e. half of the landslides of the given volume and type will travel further than this line while the 10% line (yellow) represents a 10% chance that a similar landslide will travel further (McDougall 2017).

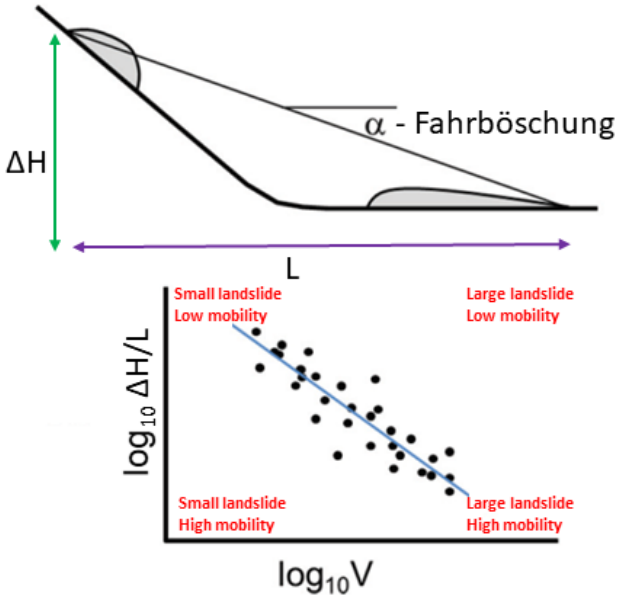

Figure 2.3 Schematic representation of the fall height (ΔH) and runout distance (L) parameters for a landslide and the conceptual relationship between ΔH/L and the landslide volume (V) (modified from McDougall 2017).

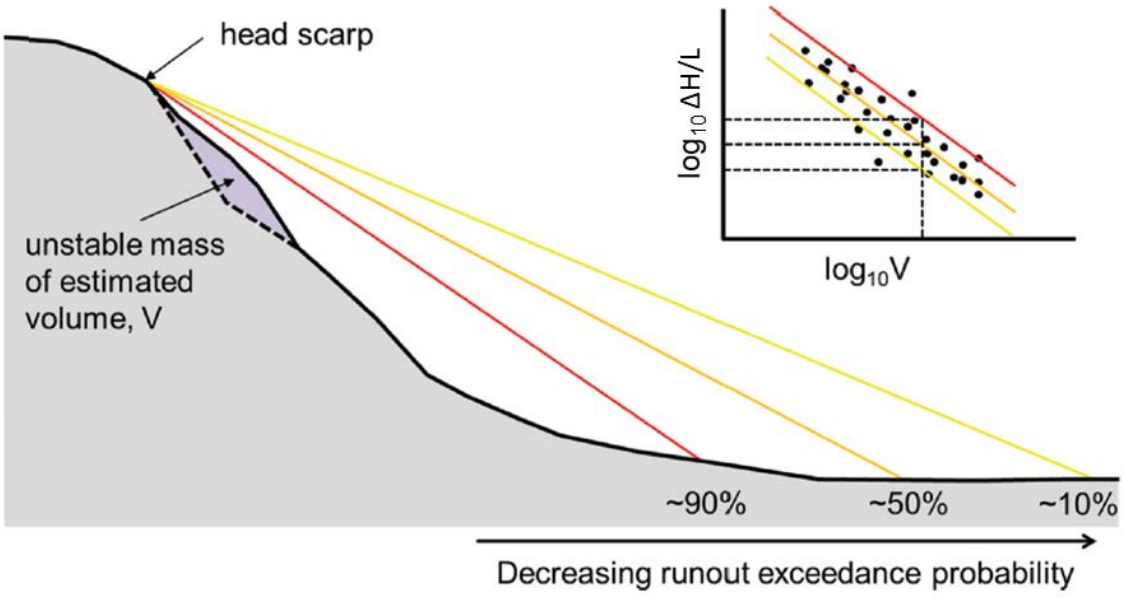

Figure 2.4 Schematic representation of runout exceedance probability based on empirical relationships (modified from McDougall 2017).

To minimise variability in empirical relationships, tools to estimate landslide runout need to be calibrated to the region-specific characteristics over which they will be applied. To address these contributing factors in the empirical runout-relationships, three plots between the ΔH/L and volume have been compiled from the relevant Kaikōura- and New Zealand-specific landslide runout information available (Figure 2.5, Figure 2.6, and Figure 2.7). The three plots represent:

1. Earthquake-triggered dry open-slope debris avalanches, which transition into rock avalanches (volume greater than 100,000 m^3) such as those landslides that were generated in greywacke rocks and other derivative materials during the 2016 Kaikōura earthquake (Figure 2.5);
2. Rainfall-triggered wet open-slope debris avalanches and debris flows such as those triggered along the Kaikōura coast during cyclones Debbie and Cook and ex-tropical cyclone Gita, and which involved the reactivation of landslides and debris generated by the Kaikōura earthquake (Figure 2.6 and Figure 2.7); and
3. Rainfall-triggered wet channelised debris flows, where the debris is predominantly confined to drainage lines/channels. All channelised landslides are assumed to be wet.

The methodology used in this project incorporates the effect of topography by using the LiDAR-derived DEM to measure the elevation and travel distance between landslide source, transport zone, and debris deposit. The methodology also accounts for channel confinement (a specific aspect of the transport zone topography) by differentiating between open-slope debris avalanches (Figure 2.5 and Figure 2.6) and channelised debris flows (Figure 2.9). It also accounts for the enhanced mobility of landslides that are over 100,000 m^3 by using an empirical relationship for rock avalanches (Figure 2.5). The best fit lines (and associated statistics) for the ΔH/L as a function of volume plots were determined using a least square method in a spreadsheet environment. Using the data is normally distributed on either side of the best fit lines, the 1%, 10%, 25%, 75%, 90% and 99% runout exceedance probability lines were calculated (Figure 2.5, Figure 2.6, Figure 2.7).

The dry debris avalanche and rock avalanche empirical relationship is intended to represent debris and rock slope failures that are associated with earthquake-triggered landslides (e.g., Port Hills and Kaikōura events) or with large volume (>100,000 m^3) rock avalanches. In this project, we assume landslides >100,000 m^3 are rock avalanches. The rationale for considering the large volume rock avalanches as dry is that they do not represent water saturated masses in the same way to rainfall-triggered debris avalanches or debris flows. The bi-linear behaviour (in log-log space) of the relationship between ΔH/L ratio and volume had previously been noted by other researchers (e.g., Scheidegger 1973; Finlay et al. 1999; Hermanns et al. 2012; Whithall 2019). In this project, rock avalanches up to 10,000,000 m^3 were considered, because the largest rock avalanche triggered during the 2016 Kaikōura earthquake was the Hapuku landslide at about 12,000,000 m^3. Table 2.2 summarises the Fahrböschung (and equivalent ΔH/L ratio) for each of the volume classes investigated in this project.

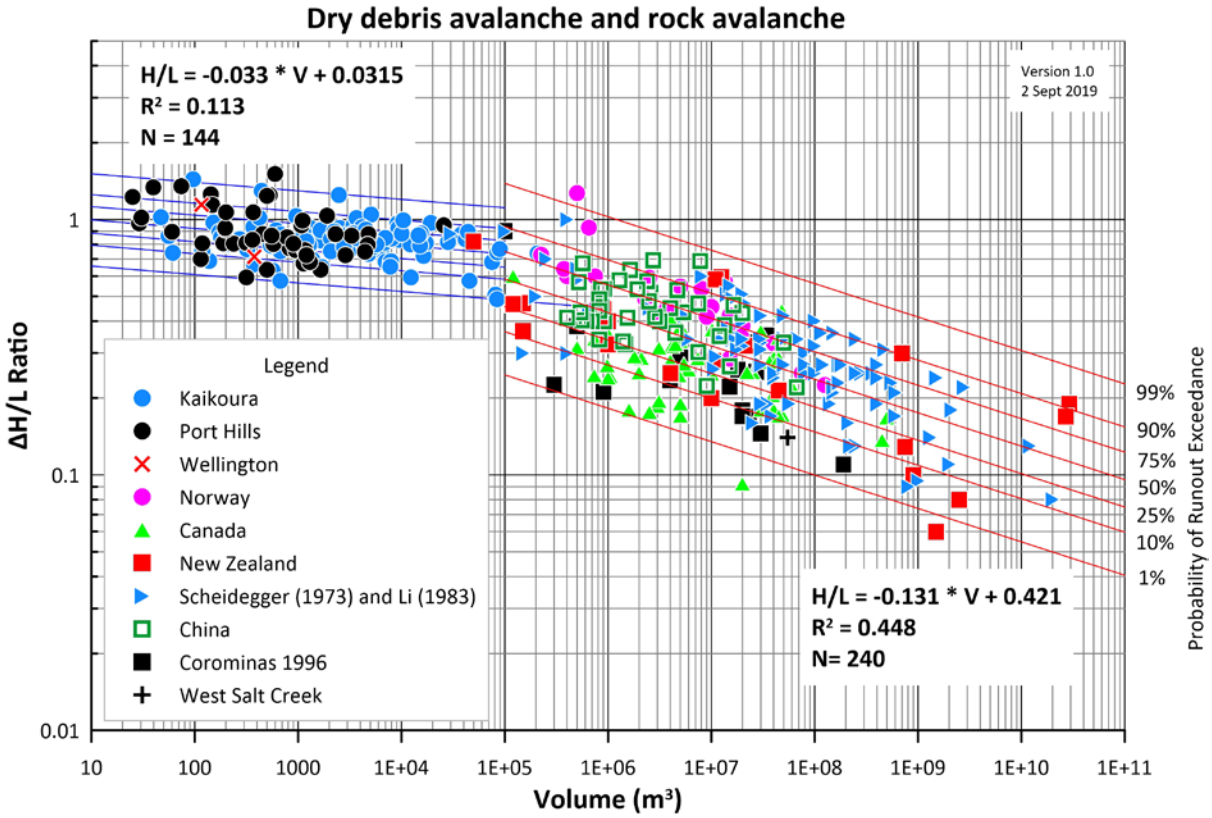

Figure 2.5 Empirical relationship between ΔH/L ratio and volume in dry (i.e., earthquake-triggered) debris avalanches (<100,000 m^3) and rock avalanches (>100,000 m^3).Table 2.2 Summary of Fahrböschung and ΔH/L value for each volume class of dry debris avalanche and rock avalanche used in this project. See Figure 2.7 for graphical representation of data considered.

Volume (m^3)	50% Runout Exceedance Probability	
	Fahrböschung (°)	ΔH/L
10	45	1.0
100	43	0.93
1000	41	0.87
10,000	38	0.78
100,000	30	0.58
1,000,000	23	0.42
10,000,000	18	0.32

Rainfall-triggered debris avalanches on open-slopes and have previously been referred to as open-slope debris flows. In this project the term debris flow is reserved for landslides travelling within a channelised path (Hungr et al. 2014). The range of source materials for the rainfall-triggered debris avalanches compiled in Figure 2.6 include till (Milne et al. 2015; Brideau et al. 2019), weathered granite (Wong et al. 1998, Hunter and Fell 2003; Wong et al. 2004) and weathered greywacke bedrock/colluvium (Kaikōura). The examples from the Kaikōura region were triggered by ex-tropical cyclone Gita. They show a wide range of mobility which upon initial review appears to be associated with the different vegetation (pasture, scrub, or mature forest) along the runout path but all the factors influencing runout mentioned earlier in this section could have contributed. As rainfall-triggered debris avalanches interact with the surficial material and/or weathered bedrock along the travel path their volumes can vary, but typically they tend to be <100,000 m^3. Table 2.3 summarises the Fahrböschung (and equivalent ΔH/L ratio) for each of the volume classes investigated in this project.

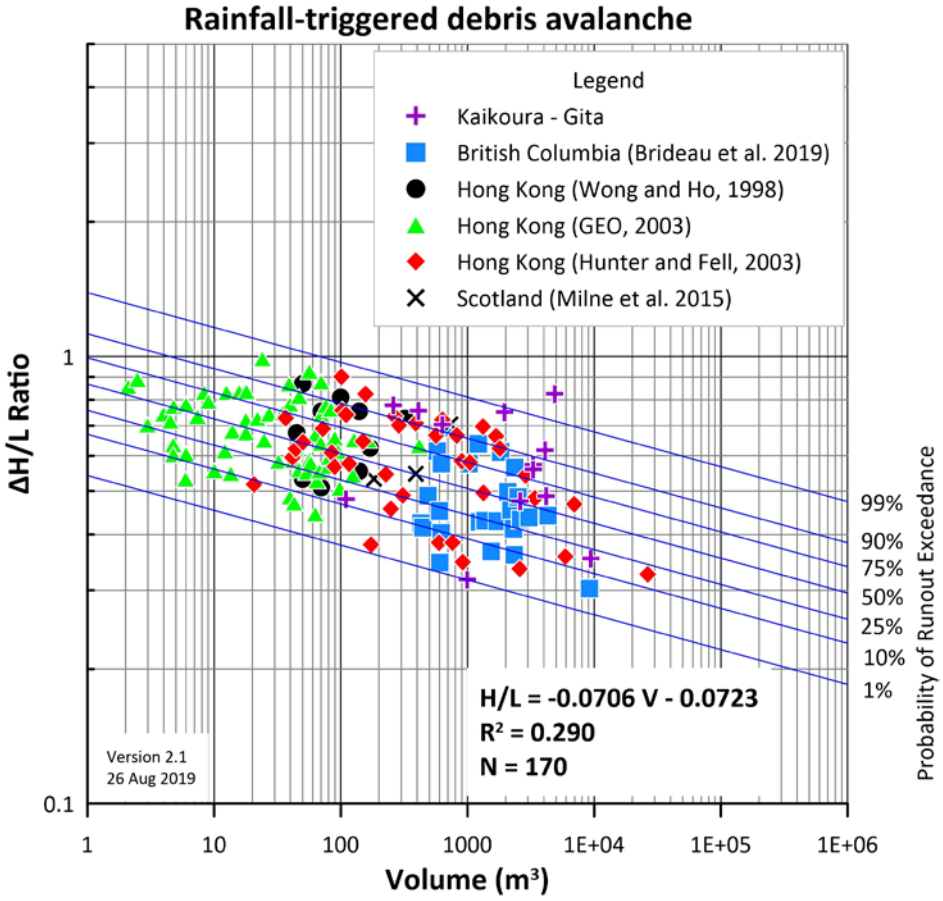

Figure 2.6 Empirical relationship between ΔH/L ratio and volume for rainfall-triggered debris avalanches (open-slope or non-channelised and sometimes previously referred to as open-slope debris flows).

Table 2.3 Summary of Fahrböschung and ΔH/L value for each volume class of rainfall-triggered debris avalanche considered in this project. See Figure 2.8 for the graphical representation of the data considered.

Volume (m^3)	50% Runout Exceedance Probability	
	Fahrböschung (°)	ΔH/L
10	36	0.73
100	32	0.62
1000	28	0.52
10,000	24	0.45
100,000	21	0.38

The rainfall-triggered debris flows compiled in this project cover a wide range of geographical areas and source materials (Figure 2.7). Debris flows initiating from volcanic edifices (i.e., lahars) were excluded as they have a documented high mobility (Griswold and Iverson 2014) and the project area contains only limited exposures of volcanic material. The range of volume categories considered for this project include up to 1,000,000 m^3, because a ~200,000 m^3 debris flow was documented during 2017 ex-tropical cyclone Gita. Table 2.4 summarises the Farhböschung (and equivalent ΔH/L ratio) for each of the volume classes investigated in this project.

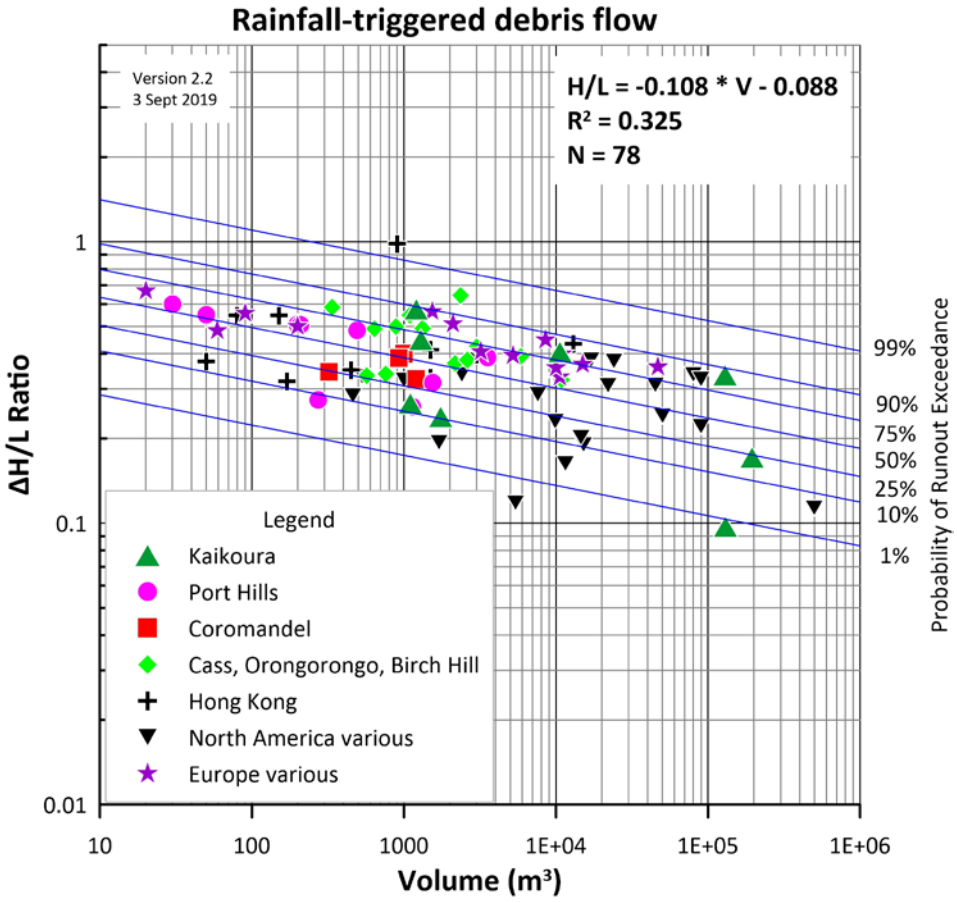

Figure 2.7 Empirical relationship between ΔH/L ratio and volume for rainfall-triggered debris flows (confined or channelised).

Table 2.4 Summary of the Fahrböschung and ΔH/L value for each volume class of rainfall-triggered debris flow considered in this project. See Figure 2.9 for graphical representation of the data considered.

Volume (m^3)	50% Runout Exceedance Probability	
	Fahrböschung (°)	ΔH/L
10	33	0.65
100	26	0.49
1000	21	0.38
10,000	17	0.31
100,000	13	0.23
1,000,000	10	0.18

2.5.2 Implementation of Empirical Runout Methodology in ArcGIS

This was done in a series of steps:

- Step 1: Identify potential landslide source areas
- Step 2: Carry out dry open-slope debris avalanche/rock avalanche runout modelling and wet debris avalanches runout modelling; and
- Step 3: Carry out channelised debris-flow runout modelling for wet flows.

2.5.2.1 Step 1: Source area identification

Identification of potential landslide source areas took place in two stages, with both stages used to define the maximum credible landslide source volume that could occur from any given slope:

1. Local slope relief (LSR): the difference between the elevation of the grid cell and the lowest point in an 80 m radius circle, projected from each grid cell. The 80 m radius value was selected to capture the representative difference in elevation of the slope of interest while minimizing situations where the relief of a neighbouring slope is getting attributed to a pixel. In this project we use a 3 m by 3 m resolution DEM resampled from the 1 m resolution DEM derived from the 2016 LiDAR survey. This LSR to volume relationship is based on 19,800 landslides that were triggered by the 2016 Kaikōura Earthquake. We used it to identify which slopes would be large enough in height (LSR) to generate landslides of a given volume (Figure 2.8). Table 2.5 summarises the LSR values assumed for each landslide volume class considered in this project. The LSR was calculated for sections of the hillside based on the elevation difference in the DEM cells within the 80 m radius that had a gradient greater than 20°. This first stage was done to avoid identifying gentle slopes (i.e., < 20°) that have a low likelihood of generating debris avalanches, rock avalanches, and debris flows.

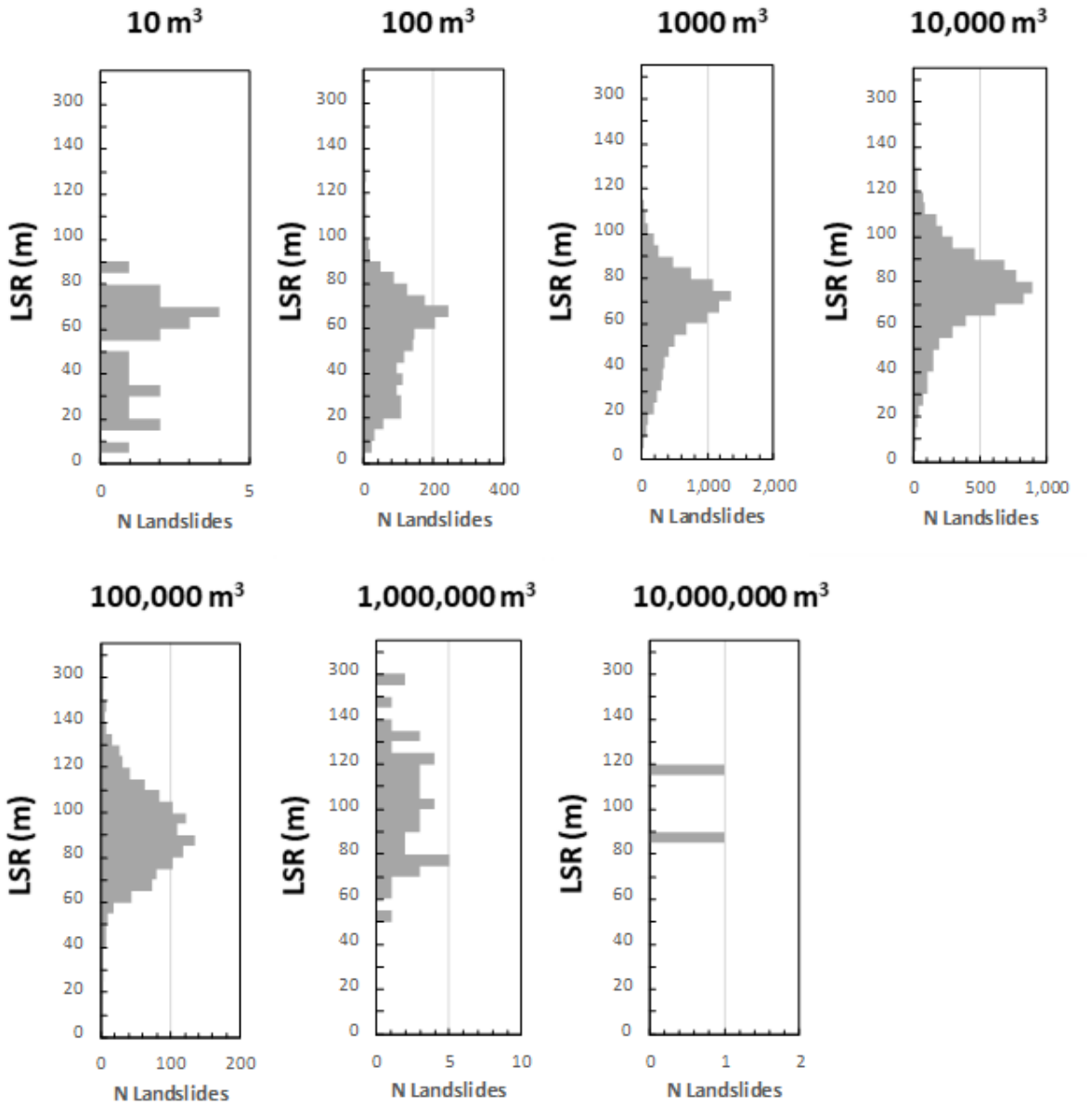

Figure 2.8 Local slope relief (LSR) for the slopes on which the different volume classes of landslides triggered by the Kaikōura Earthquake occurred. N landslides = 19,800.

Table 2.5 Summary of the estimated potential landslide source volume as a function of the local slope relief calculated in the 80 m radius.

Volume bin range (m^3)	Representative volume (m^3)	Minimum local slope relief in the 80 m radius (m)
1–10	10	3
>10–100	100	22
>100–1000	1000	39
>1000–10,000	10,000	51
>10,000–100,000	100,000	66
>100,000–1,000,000	1,000,000	71
>1,000,000	10,000,000	83

2. The landslide source area: we used the landslide source volume and area relationship derived for 13,500 landslides, mainly debris avalanches in greywacke, triggered by the 2016 Kaikōura earthquake (Figure 2.9 and Table 2.6; Massey et al. in review). These areas were used to screen (remove) slopes not large enough to generate a landslide of a given volume class.

This two-stage process allowed slopes which could potentially generate landslides up to a given source volume to be systematically identified within the project area. This is important because larger landslides generally result in longer landslide debris inundation zones. The location of each potential 10,000,000 m^3 and 1,000,000 m^3 landslide source was assessed manually to ensure such slopes could credibly generate such large landslides. Spot checks were done on smaller slopes only able to generate smaller landslides.

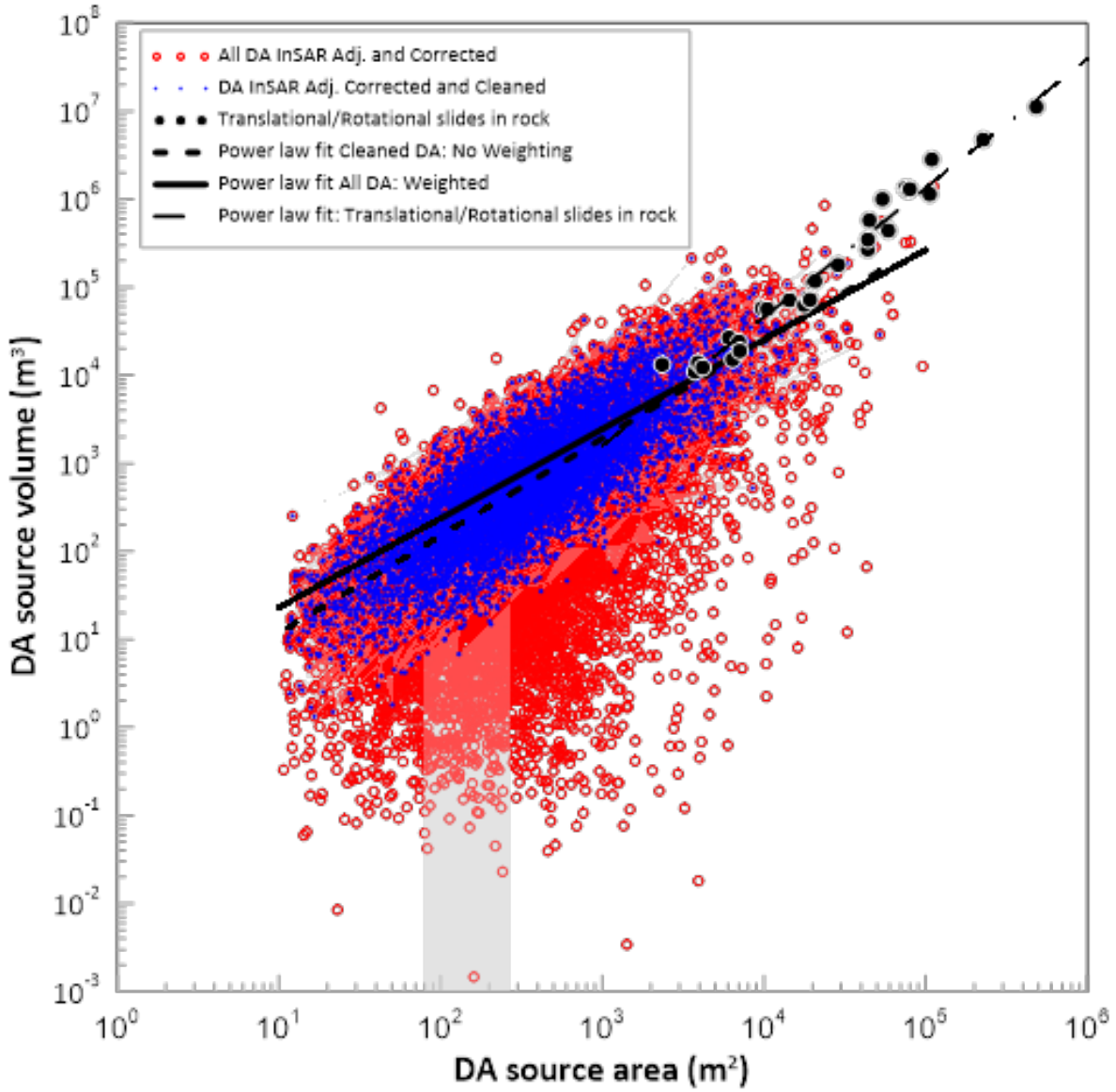

Figure 2.9 Empirical relationship between landslide source plan area and the landslide volume as derived for the debris avalanches (DA) triggered by the 2016 Kaikōura Earthquake in the greywacke-dominated terrain (GeolCode4). From Massey et al. (in review).

Table 2.6 Empirical relationship between the landslide source plan area and the landslide volume for greywacke-dominated terrain that was used to validate the potential landslide source area used in the empirical runout model. Values are derived from relationship in Massey et al. (in review).

Volume bin range (m^3)	Mean source area for volume bin range (m^2)	Representative Landslide volume (m^3)	Source plan area (m^2) for representative landslide volume from fit in Figure 2.9
1–10	<32	10	5
>10–100	32	100	45
>100–1000	460	1000	410
>1000–10,000	1300	10,000	3800
>10,000–100,000	4700	100,000	35,000
>100,000–1,000,000	21,000	1,000,000	371,000
>1,000,000	Limited data	10,000,000	2,900,000

2.5.2.2 Step 2: Open-slope runout modelling

To estimate the runout distance of the open-slope landslides, GNS Science developed a GIS script that combines the Fahrböschung method with methodology used in the ArcGIS Visibility Tool. The visibility tool assesses which areas can be seen from a particular location. In this project, for each landslide volume class, the elevation of a grid cell within the source was projected in eight directions (i.e., to each adjacent grid cell) using the Fahrböschung. This projected elevation was compared with the elevation obtained from the DEM. All the cells with the projected elevation above the DEM were considered to be 'visible' and within the inundated area, but only if they were downhill from the processing cell. The process was continued using these inundated cells as sources until no more cells were inundated (Figure 2.10A). To avoid the landslide runout stopping when reaching a small step in elevation, especially for larger volumes (1000 m^3 or greater), an allowed arbitrary obstacle height (Table 2.7) was introduced and subtracted from the DEM when the downhill cells were determined (Figure 2.10B). The 3 m resolution DEM is used for processing and the Fahrböschung for each landslide volume class is listed in Table 2.2 (dry) and Table 2.3 (wet).

Table 2.7 Height of the topographic obstacle that was assumed to not affect the runout of a debris avalanche per landslide volume class.

Landslide volume class (m^3)	Obstacle height that does not stop runout (m)
10, 100	0
1000	0.5
10,000, 100,000, 1,000,000, 10,000,000	1

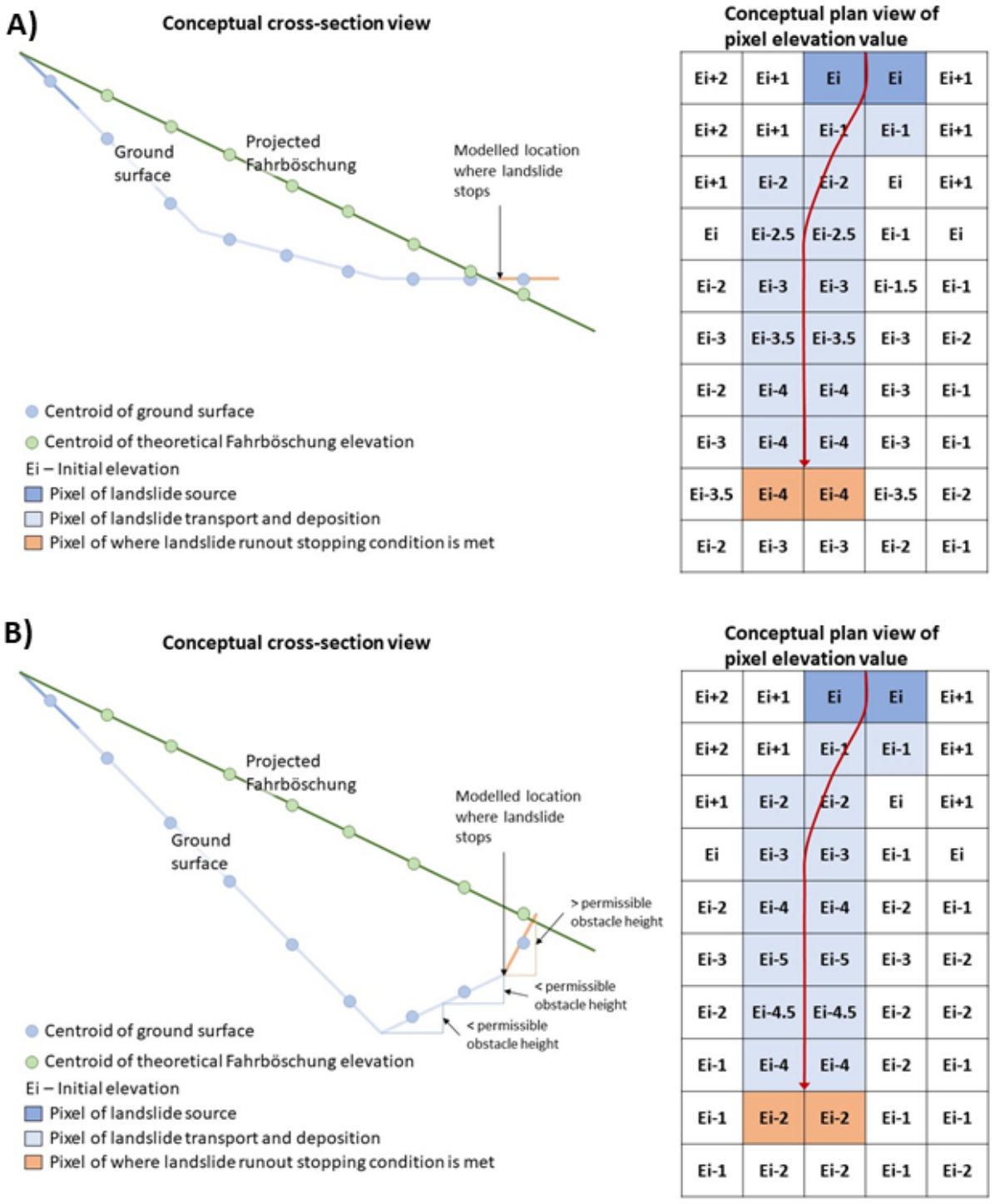

Figure 2.10 Conceptual representation of the landslide runout model stopping rules as implemented in GIS. A) the modelled travel path (red arrow) intersects the Fahrböschung for the landslide volume class investigated, and B) the modelled travel path exceeds the obstacle size defined for the landslide volume class investigated.

Step 3: Channelised runout modelling

To estimate the runout distance of the channelised flows, GNS Science developed a GIS script that uses the same method as described above, but where the source elevations were projected cell by cell only downhill, along the steepest flow path from each cell.

No obstacles were allowed in this model, so it was necessary to 'fill' the DEM to remove artificial 'sinks' on the assumption that all the sinks are artefacts of the DEM generation process. A flow direction grid was generated to establish the potential runout path from each grid cell and elevations were projected only along these paths using Fahrböschung for each landslide volume class (Table 2.4).

2.6 Field Verification

Two days of field verification of the fan delineation and landslide debris inundation mapping were conducted on 28 and 29 August 2019 by Marc-André Brideau and Chris Massey, both of GNS Science. Field verification focused on three pilot study areas near Kekerengu, Mangamaunu, and Oaro (Figure 1.1). These areas were selected to cover a range of geological material (Table 2.8), topography, landslide volumes, and landslide runouts in the Kaikōura District.

Table 2.8 Geological units from the Edbrooke et al. (2015) compilation in the three pilot study areas that were part of the field verification for this project.

Geological unit	Age	Main lithologies
Motunau Group	Miocene	Calcareous sandstone, siltstone and mudstone with bioclastic limestone
Muzzle Group	Palaeocene-Eocene	Siliceous micritic limestone with siltstone
Eyre Group	Late Cretaceous	Siltstone, sandy mudstone, sandstone
Coverham Group	Early Cretaceous	Moderately indurated conglomerate, sandstone, siltstone
Pahau Terrane	Early Cretaceous	Greywacke (sandstone and mudstone)

During field verification, small fans were also examined in the town of Kaikōura to assess whether their location in an urban environment could result in a higher susceptibility to generate damage to property. The large debris-flow fans on the southern face of Mount Fyffe were also visited to calibrate the mapped extent of the fans.

The main finding from the field verification was that the potential landslide source volumes were being overestimated when using only the LSR criteria (Figure 2.8 and Table 2.5). These preliminary results indicated that the identified potential landslide sources needed a second assessment criteria, the area to volume relationship shown in Figure 2.9. These findings were incorporated into the methodology in Section 2.5.2.1.

3.0 RESULTS

3.1 Fan Delineation

A total of 253 fans were identified in the project area. Fans were delineated for catchments with stream order 3 or less (Section 3.2). Catchments of order greater than 3 were assumed to be dominated by fluvial processes. Figure 3.1 presents histograms of the mapped fan area. While most of the fans have an area less than 5000 m^2 (Figure 3.1B), there is a second grouping with area larger than 100,000 m^2 (Figure 3.1C). Attributes of each fan include their fan area, catchment order, catchment area, catchment length, and Melton Ratio of the catchment. The extent and location of the fans identified as part of this project are provided to CRC and KDC as an ArcGIS shapefile.

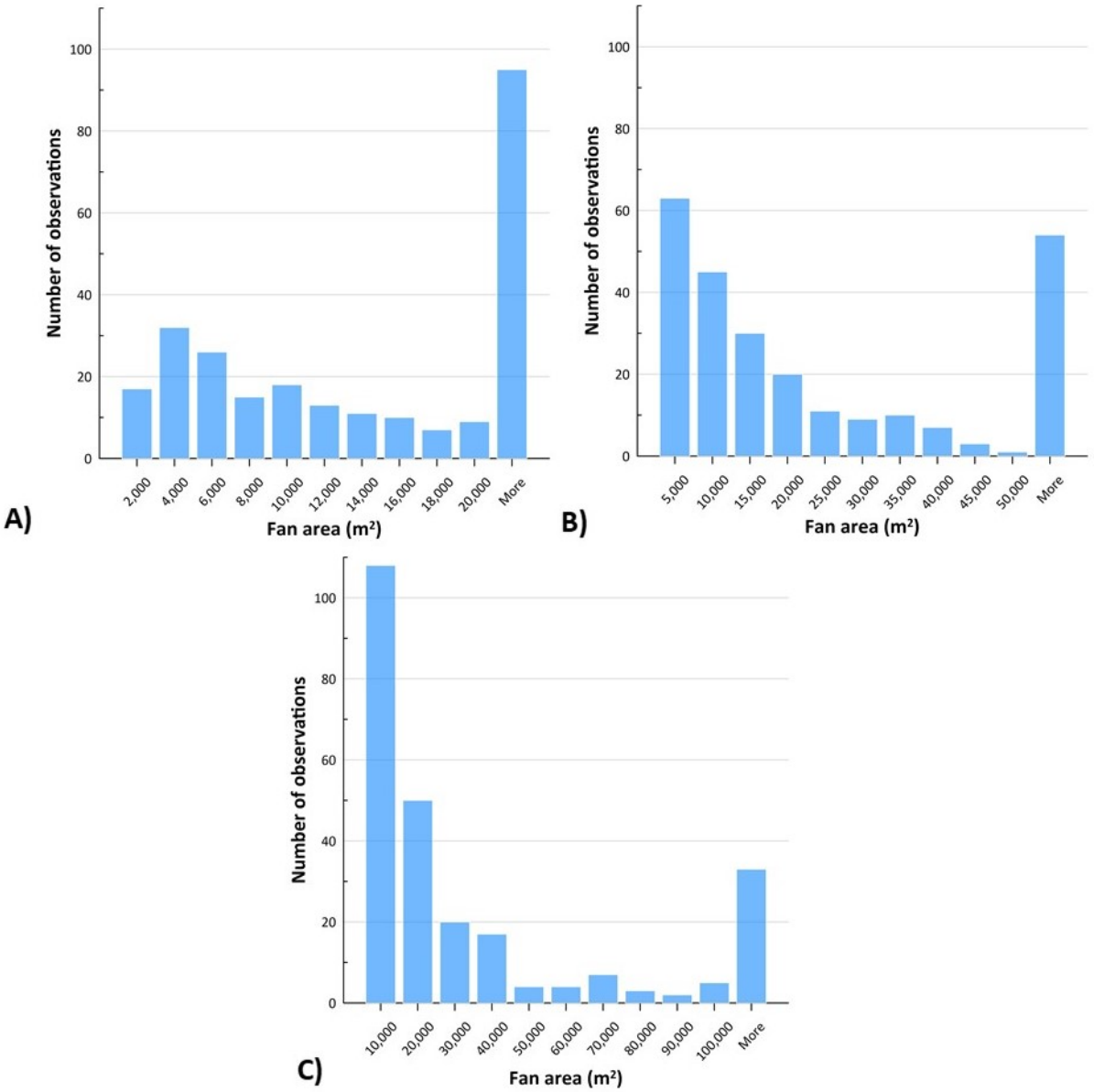

Figure 3.1 Histograms of the mapped fan area for this project using A) 2000 m^2, B) 5000 m^2, and C) 10,000 m^2 bin sizes. Note that while vertical bar plots on the tick mark of a bin size it represents fan sizes less than that bin size. For example, in panel C) the bar at 10,000 m2 represents fans with an area less than 10,000 m^2 while the vertical bar at 20,000 m^2 represents fans with areas between 10,000 and 20,000 m^2.

3.2 Melton Ratio and Catchment Length

The distribution of catchment length and Melton Ratio for the 253 fans mapped in the project area is presented in Figure 3.2 as a function of the catchment order and length. The three fields showing which process dominates are outlined in Figure 3.2; these are based on the empirical values for the catchment length and Melton Ratio listed in Table 2.1. These values were selected based on the work of Wilford et al. (2004) with the modification by Welsh and Davies (2011) based on their observations of landslides in the Coromandel Peninsula (i.e., Melton Ratio of 0.5 instead of 0.6 as the boundary between debris flow and debris flood). Figure 3.2 shows that as the catchment order increases, it tends to be dominated by flooding (fluvial) processes.

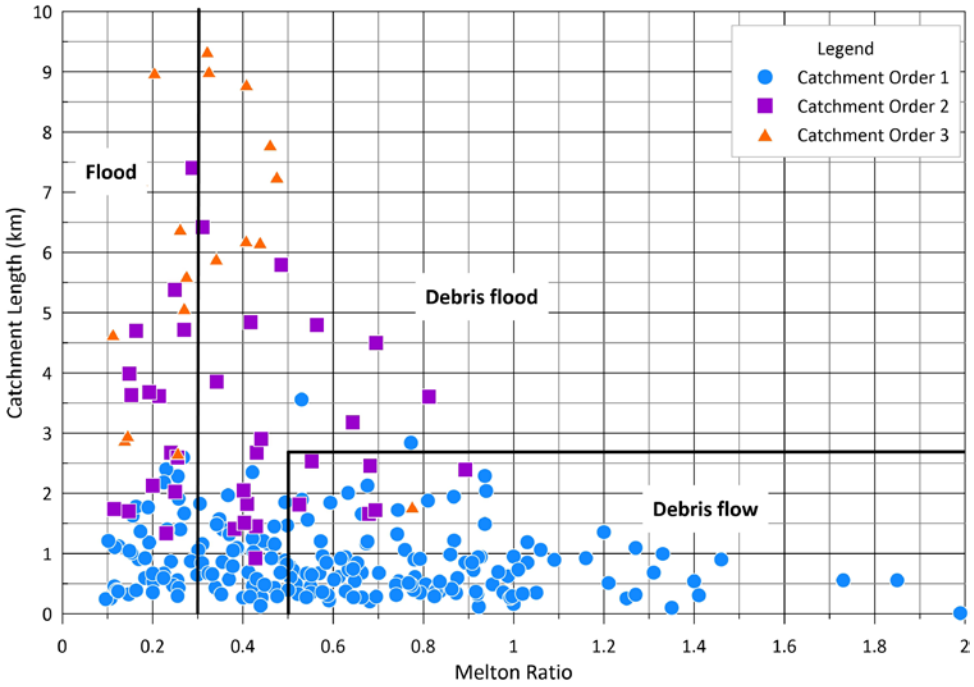

Figure 3.2 Plot of the catchment length and Melton Ratio for catchments in the project area that have a stream order of 3 or less. Fields of flood, debris flood, and debris flow dominated catchments are based on the criteria from Wilford et al. (2004) with modification by Welsh and Davies (2011) based on New Zealand case studies.

3.3 Open-Slope Landslide Debris Inundation

A section of the Kowhai River Valley is shown in Figure 3.3 (dry earthquake-triggered) and Figure 3.4 (wet rain-triggered) as examples of the estimated open-slope landslide debris inundation models. Figure 3.3 and Figure 3.4 show the modelled source volumes and the associated debris inundation for each volume class. As anticipated from the observed empirical relationships (Section 2.5.1), with the progressive addition of larger volume classes in each panel (Figure 3.3 and Figure 3.4) the modelled areas inundated by debris increase. Figure 3.4 also demonstrates that wet open-slope landslides travel further than dry open-slope landslides (Figure 3.3) of a similar volume. It should be emphasised that Figure 3.3 and Figure 3.4 represent the runout from every source identified and that during an earthquake or intense rainfall event not every potential source would generate a landslide. For example, Figure 2.10 shows that during the 2016 Kaikōura Earthquake only two 10,000,000 m^3 landslides occurred.

The potential landslide source location and modelled debris inundation extent for the dry and wet open-slope landslides for the whole project area are provided to CRC and KDC as ArcGIS shapefiles.

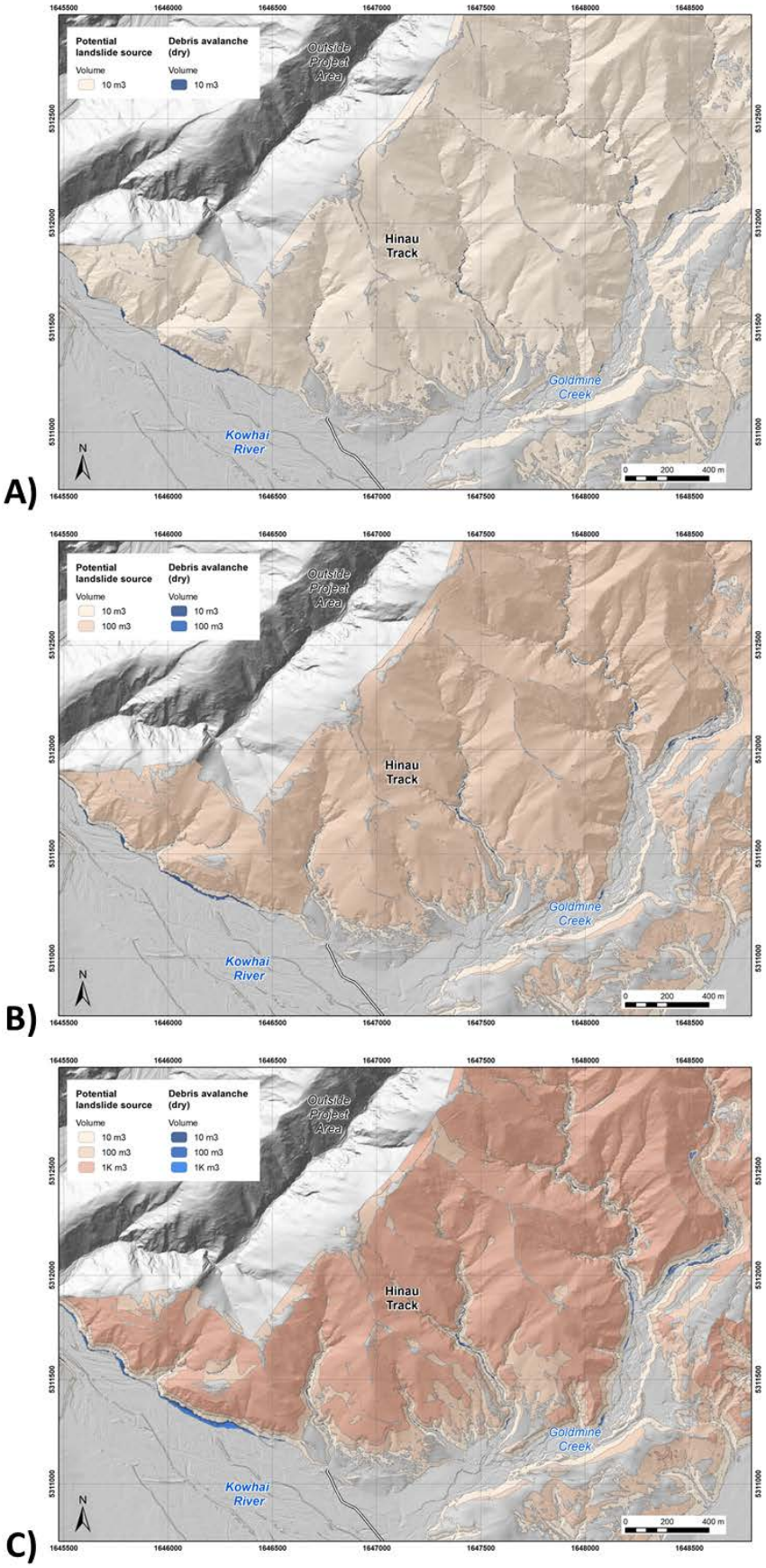
A)
Potential landslide source
Volume
10 m3
Debris avalanche (dry)
Volume
10 m3
Outside Project Area
Hinau Track
Goldmine Creek
Kowhai River
N
0 200 400 m
B)
Potential landslide source
Volume
10 m3
100 m3
Debris avalanche (dry)
Volume
10 m3
100 m3
Outside Project Area
Hinau Track
Goldmine Creek
Kowhai River
N
0 200 400 m
C)
Potential landslide source
Volume
10 m3
100 m3
1K m3
Debris avalanche (dry)
Volume
10 m3
100 m3
1K m3
Outside Project Area
Hinau Track
Goldmine Creek
Kowhai River
N
0 200 400 m

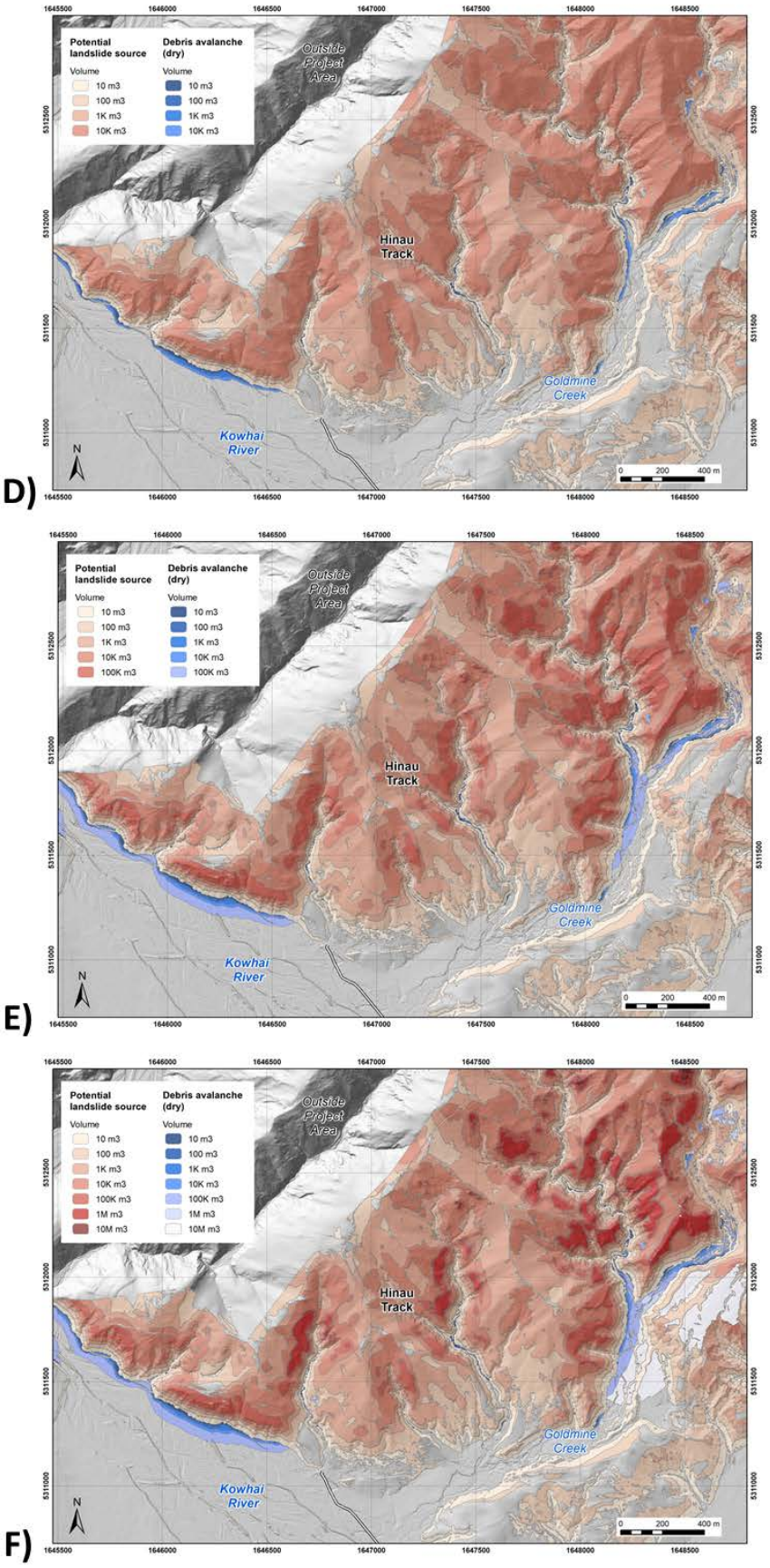

Figure 3.3 Section of the Kowhai River Valley providing an example of the modelled landslide debris inundation for dry open-slope debris avalanches and rock avalanches. Plot showing the modelled source (warm colours) and runout (cool colours) for A) 10 m^3, B) 100 m^3, C) 1000 m^3, D) 10,000 m^3, E) 100,000 m^3, and F) 1,000,000 and 10,000,000 m^3.

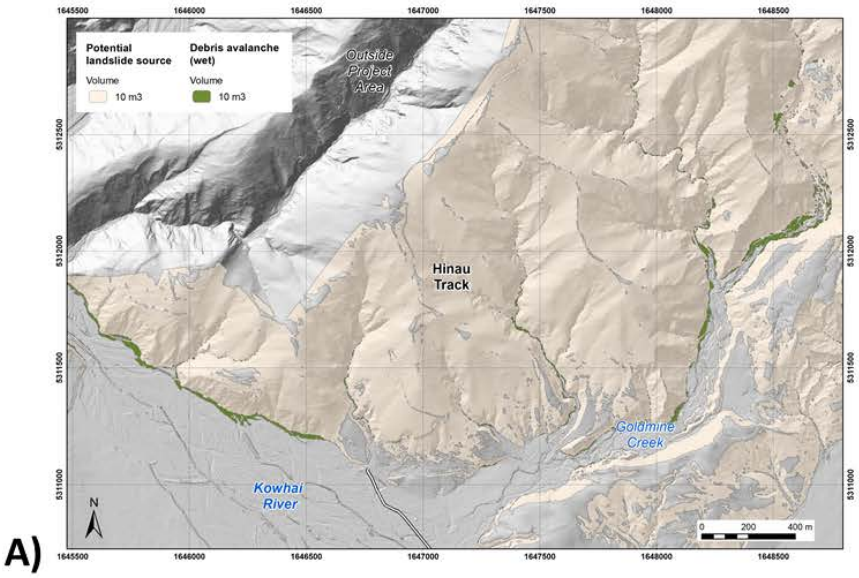
A)
Potential landslide source
Volume
10 m3
Debris avalanche (wet)
Volume
10 m3
Outside Project Area
Hinau Track
Goldmine Creek
Kowhai River
N
0 200 400 m
1645500 1646000 1646500 1647000 1647500 1648000 1648500
5312500 5312000 5311500 5311000

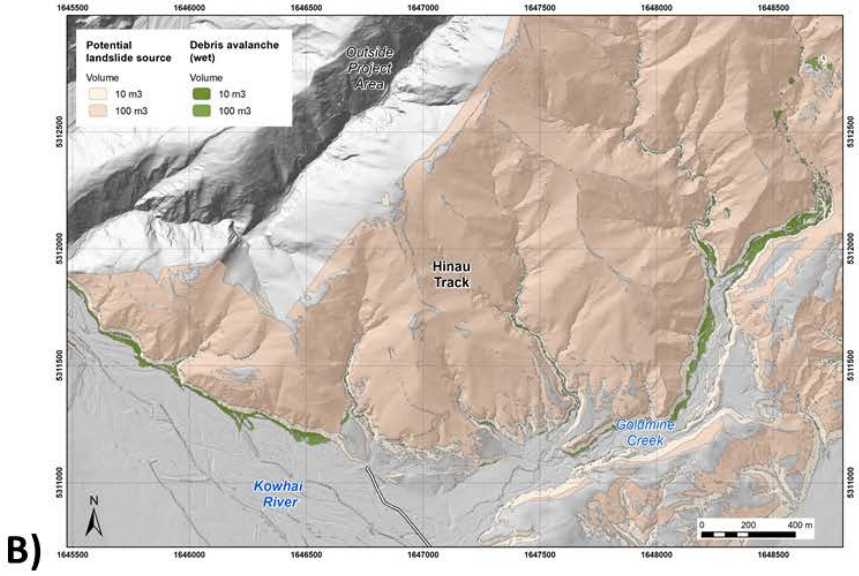
B)
Potential landslide source
Volume
10 m3
100 m3
Debris avalanche (wet)
Volume
10 m3
100 m3
Outside Project Area
Hinau Track
Goldmine Creek
Kowhai River
N
0 200 400 m
1645500 1646000 1646500 1647000 1647500 1648000 1648500
5312500 5312000 5311500 5311000

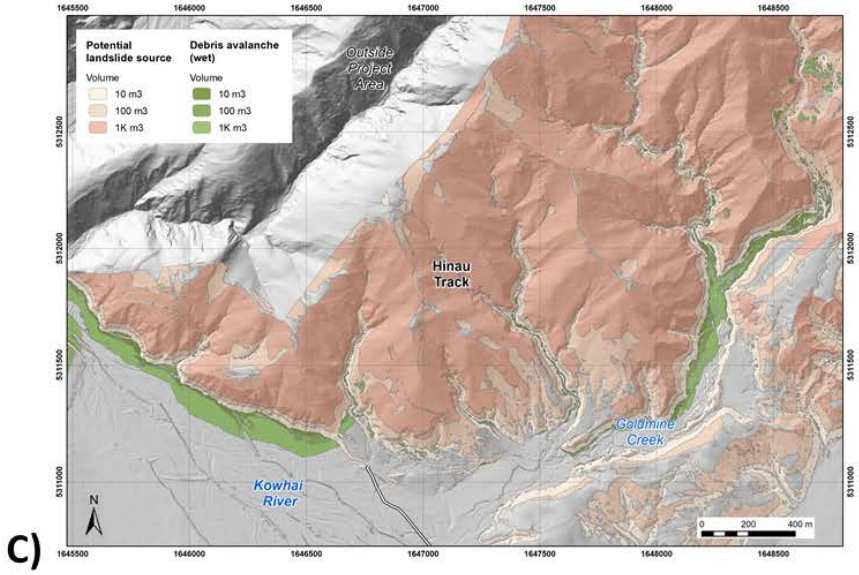
C)
Potential landslide source
Volume
10 m3
100 m3
1K m3
Debris avalanche (wet)
Volume
10 m3
100 m3
1K m3
Outside Project Area
Hinau Track
Goldmine Creek
Kowhai River
N
0 200 400 m
1645500 1646000 1646500 1647000 1647500 1648000 1648500
5312500 5312000 5311500 5311000

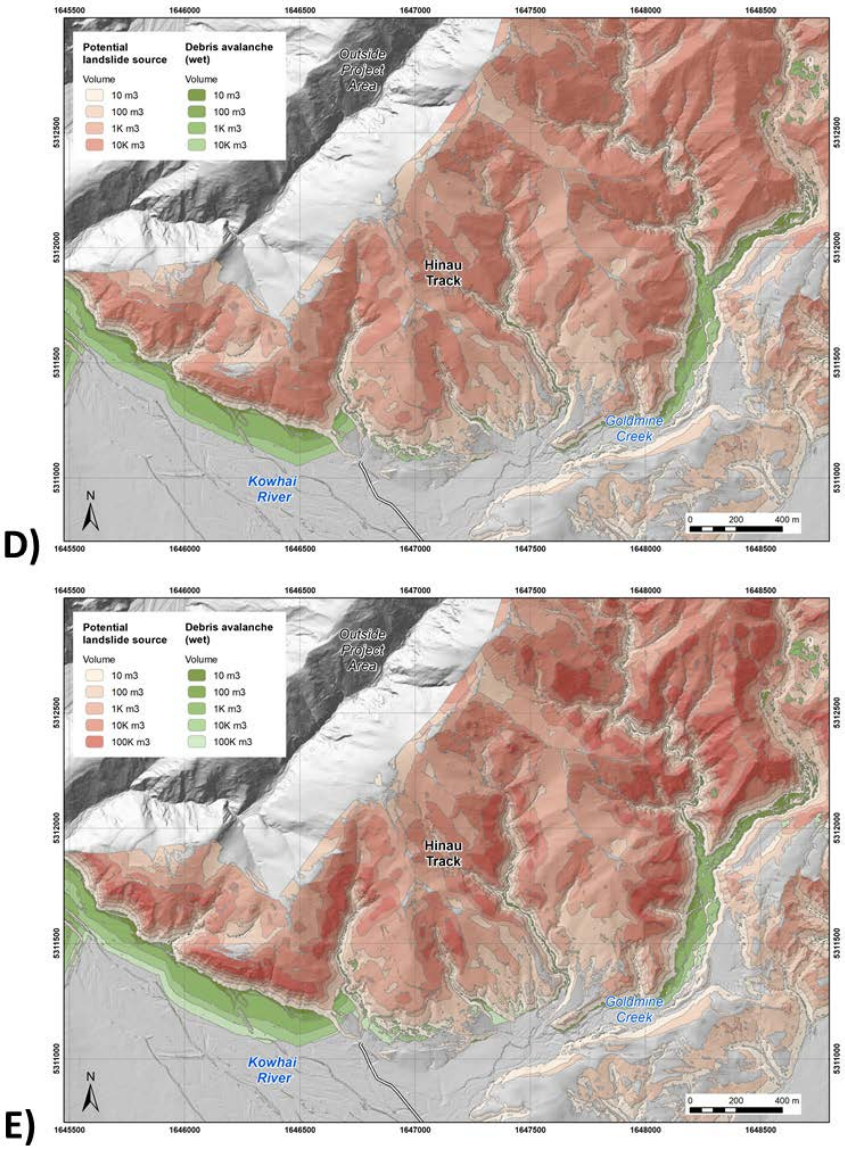

Figure 3.4 Section of the Kowhai River Valley providing an example of the modelled landslide debris inundation for wet open-slope debris avalanches. Plot showing the modelled source (warm colours) and runout (greens) for A) 10 m^3, B) 100 m^3, C) 1000 m^3, D) 10,000 m^3, and E) 100,000 m^3.

3.4 Channelised Landslide Debris Inundation

A section of the Kowhai River Valley is shown in Figure 3.5 as an example of the results from the modelled wet channelised debris-flow inundation.

Whereas the open-slope landslide inundation models covered the entire project area, the outputs of the wet channelised debris-flow inundation modelling are only reported for the 253 mapped fans. This assumes that landslide debris inundation outside of the mapped fans is captured by the open-slope landslide debris inundation models (Section 3.3). The extent of the channelised debris-flow inundation is shown by a line on the fan for each debris-flow volume class modelled. These lines, indicating debris-flow inundation extent, are extrapolated across the width of the fan to account for potential avulsion of the active channel (Figure 3.5).

The estimated debris-flow inundation lines on the mapped fans are provided to CRC and KDC as an ArcGIS shapefile.

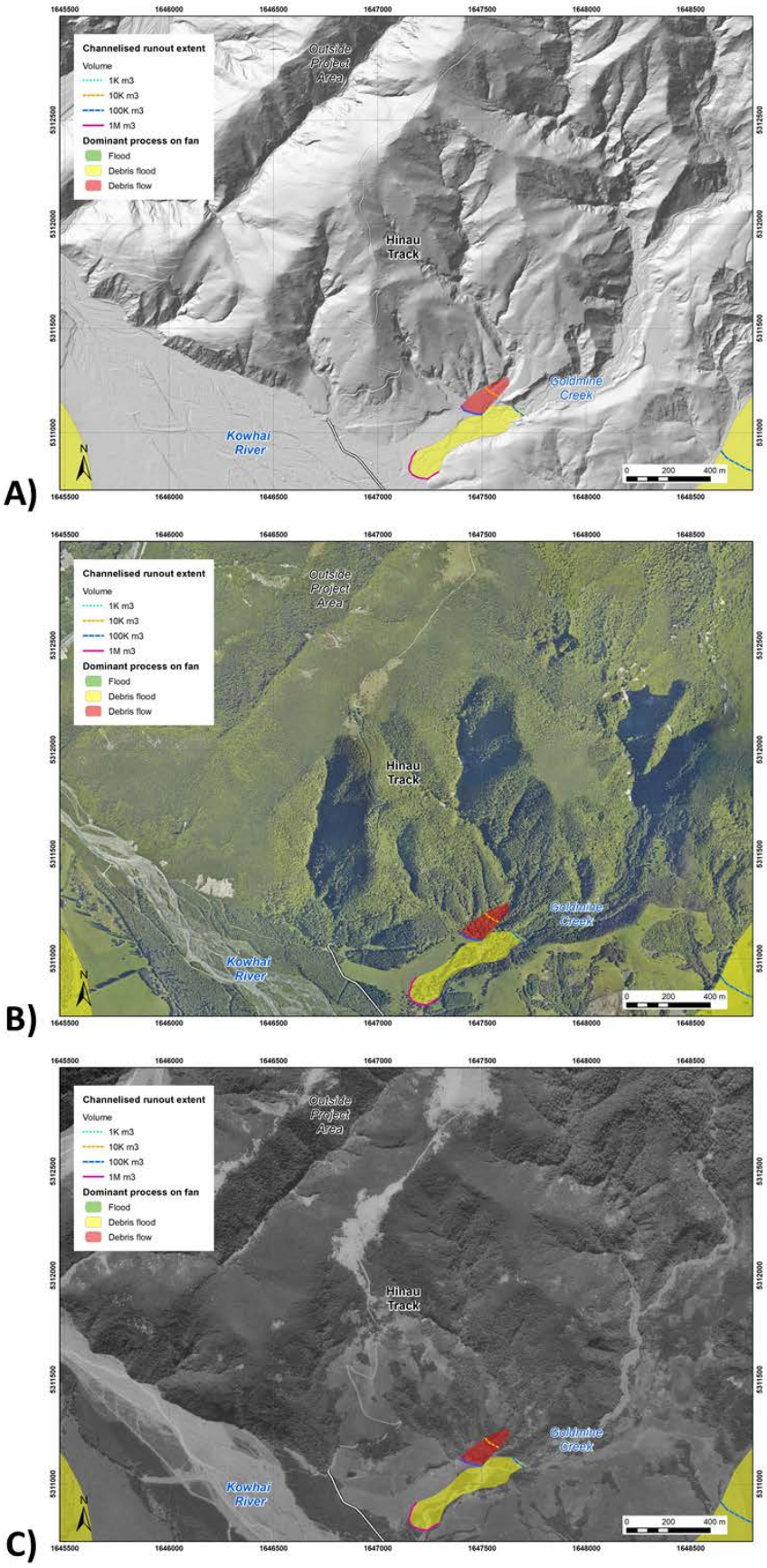

Figure 3.5 Section of the Kowhai River Valley providing an example of the modelled landslide debris inundation for wet channelised debris flows with a A) hillshade model from the 2016 post-earthquake LiDAR, B) 2016 post-earthquake aerial photograph, and C) 1975 post-cyclone Alison aerial photograph as background imagery. Fans are symbolised based on dominant hazard process identified using the Melton Ratio and catchment length (Section 2.3).

4.0 SUMMARY AND RECOMMENDATION

This Phase 1, report provides a district-scale deterministic assessment of the locations within the project area that could be affected by debris and rock avalanches (slippage and falling debris) and debris flows (debris-flow fans) triggered by earthquakes and rain. The landslide debris inundation areas were modelled in ArcGIS using a set of empirical relationships based on observations of landslides from New Zealand and worldwide. The landslide debris inundation modelling was carried out for three landslide types: 1) debris flows; 2) debris avalanches; and 3) rock avalanches. The ArcGIS data files for the entire project area were provided to CRC and KDC.

The landslide debris inundation area was estimated for dry and wet debris avalanches (10 to 100,000 m^3) and dry rock avalanches (100,000 and 10,000,000 m^3) over the entire project area. This project also outlined the extent of 253 fans and provided a scoping-level assessment of the likely dominant process active on each fan (debris flow, debris flood, or flood) based on empirical observations from New Zealand and Canada. The landslide debris inundation from debris flows triggered by rainfall was estimated for the 253 fans mapped in the project area. The current work excluded hazards associated with fluvial floods, landslide-dam outburst floods, rock falls, and slow-moving landslides.

Results from this project highlighted that rainfall-triggered landslides (wet debris avalanches and debris flows) have a greater mobility and travel further than earthquake-triggered landslides (dry debris avalanches) of similar volume. These results are consistent with research by others in New Zealand and worldwide. This project also provided information which could be used to delineate areas with greater potential for landslide debris inundation (i.e. located downslope from potential landslide sources and within modelled runout distances based on empirical relationships).

Due to the deterministic nature of the assessment presented in this report, it does not provide a probability of occurrence for the landslide hazard scenarios considered, which would be determined in Phase 2 of this report. This means that while estimates of landslide debris inundation are available for a range of landslide types and volumes, the current work does not provide information regarding the likelihood of a given area being inundated with debris. The likelihood of a given area being inundated by debris will depend, amongst other factors, on the likelihood of the trigger occurring (recurrence interval of rainfall events and earthquakes), likelihood of landslide initiating at a particular location (site specific conditions such as geology, fracturing of the rock, and seepage), likelihood of an event of that volume occurring at that location (large landslides occur less often than small ones), cumulative likelihood of area being inundated considering landslides of different volumes (most landslide volumes make it to base of slope but fewer make it a given distance from the base of the slope). It is recommended that KDC and CRC assess whether the results from this Phase 1 study provide sufficient information to underpin District Plan provisions. The Phase 2 work would take the results from Phase 1, and estimate the spatial probability of landslides of different volumes impacting the different areas within the hazard zones identified in Phase 1. Whilst we understand that this Phase 2 work may not be needed, it would provide a more robust analysis of the landslide hazards within the district.

5.0 ACKNOWLEDGEMENTS

The authors would like to acknowledge reviews by Professor Tim Davies (University of Canterbury), Dr. Saskia de Vilder (GNS Science), and Sally Dellow (GNS Science).

6.0 REFERENCES

Brideau M-A, Stead D, Millard T, Ward B. 2019. Field characterisation and numerical modelling of debris avalanche runout on Vancouver Island, British Columbia, Canada. *Landslides*. 16:875-891. doi:10.1007/s10346-019-01141-7.

Chen H, Crosta GB, Lee CF. 2006. Erosional effects on runout of fast landslides, debris flows and avalanches: a numerical investigation. *Géotechnique*. 56(5):305-322. doi:10.1680/geot.2006.56.5.305.

Christen M, Bühler Y, Bartelt P, Leine R, Glover J, Schweizer A, Graf C, McArdell B, Gerber W, Deubelbeiss Y, et al. 2012. Integral hazard management using a unified software environment. In: *12th Congress Interpraevent*; 2012 Apr 23-26; Grenoble, France. Klagenfurt (AT): International Research Society. p. 77-86.

Corominas J. 1996. The angle of reach as a mobility index for small and large landslides. *Canadian Geotechnical Journal*. 33(2):260-271. doi:10.1139/t96-005.

Davies TR, McSaveney MJ. 2008. Principles of sustainable development on fans. *Journal of Hydrology (New Zealand)*. 47(1):43-65.

de Scally FA, Owens IF. 2004. Morphometric controls and geomorphic responses on fans in the Southern Alps, New Zealand. *Earth Surface Processes and Landforms*. 29(3):311-322. doi:10.1002/esp.1022.

Edbrooke SW, Heron DW, Forsyth PJ, Jongens R. 2015. Geological map of New Zealand. Lower Hutt (NZ): GNS Science. 2 maps, scale 1:1,000,000. (GNS Science geological map; 2).

ESRI. 2018. ArcMap Release 10.5.1. Redlands (CA): ESRI Inc.

Evans SG. 2001. Landslides. In: Brooks GR, editor. *Synthesis of Geological Hazards in Canada*. Ottawa (ON): Geological Survey of Canada. p. 43-79. (Bulletin / Geological Survey of Canada; 548).

Evans SG, Hungr O, Enegren EG. 1994. The Avalanche Lake rock avalanche, Mackenzie Mountains, Northwest Territories, Canada: description, dating, and dynamics. *Canadian Geotechnical Journal*. 31(5):749-768. doi:10.1139/t94-086.

Griswold JP, Iverson RM. 2008. Mobility statistics and automated hazard mapping for debris flows and rock avalanches. Version 1.1, April 2014. Reston (VA): U.S. Geological Survey. Scientific Investigations Report 2007-5276.

Heim A. 1932. Landslides & human lives = Bergsturz und Menschenleben. Skermer N, translator. Vancouver (BC): BiTech Publishers. 195 p.

Hermanns RL, Oppikofer T, Anda E, Blikra LH, Bohme M, Bunkholt H, Crosta GB, Dahle H, Devoli G, Fisher L, et al. 2012. Recommended hazard and risk classification system for large unstable rock slopes in Norway. Trondheim (NO): Norges Geologiske Undersokelse. Report 2012.029.

Hungr O, McDougall S. 2009. Two numerical models for landslide dynamic analysis. *Computers & Geosciences*. 35:978-992. doi:10.1016/j.cageo.2007.12.003.

Hunter G, Fell R. 2003. Travel distance angle for "rapid" landslides in constructed and natural soil slopes. *Canadian Geotechnical Journal*. 40(6):1123-1141. doi:10.1139/t03-061.

Iverson RM. 2014. Debris flows: behaviour and hazard assessment. *Geology Today*. 30(1):15-20. doi:10.1111/gto.12037.

Iverson RM, Reid ME, Logan M, LaHusen RG, Godt JW, Griswold JP. 2011. Positive feedback and momentum growth during debris-flow entrainment of wet bed sediment. *Nature Geoscience*. 4(2):116-121. doi:10.1038/ngeo1040.

Jakob M, Weatherly H, Bale S, Perkins A, MacDonald B. 2017. A Multi-Faceted Debris-Flood Hazard Assessment for Cougar Creek, Alberta, Canada. *Hydrology*. 4(1):7.

Li T. 1983. A mathematical model for predicting the extent of a major rockfall. *Zeitschrift fur Geomorphologie*. 27(4):473-482.

LINZ (Land Information New Zealand) 2012. NZ 8 m Digital Elevation Model (2012). https://data.linz.govt.nz/layer/51768-nz-8m-digital-elevation-model-2012/

Loew S, Gschwind S, Gischig V, Keller-Signer A, Valenti G. 2016. Monitoring and early warning of the 2012 Preonzo catastrophic rockslope failure. *Landslides*. 14:141-154. doi:10.1007/s10346-016-0701-y

Massey CI, Townsend DB, Rathje E, Allstadt KE, Lukovic B, Kaneko Y, Bradley B, Wartman J, Jibson RW, Petley DM, et al. 2018. Landslides triggered by the 14 November 2016 Mw 7.8 Kaikoura earthquake, New Zealand. *Bulletin of the Seismological Society of America*. 108(3B):1630-1648. doi:10.1785/0120170305.

Massey CI, Townsend D, Lukovic B, Jones K, Rhoades D, Morgenstern R, Rosser B, Ries W, Howarth J, Hamling I, et al. Landslide volume-area relationships for earthquakes are controlled by their type/failure mode and source material (in review). *Journal of Geophysical Research Earth Surface*.

McDougall S. 2017. Landslide runout analysis - current practice and challenges. *Canadian Geotechnical Journal*. 54(5):605-620. doi:10.1139/cgj-2016-0104.

Melton MA. 1965. The geomorphic and paleoclimatic significance of alluvial deposits in Southern Arizona. *The Journal of Geology*. 73(1):1-38.

Milne FD, Brown MJ, Davies MCR, Cameron G. 2015. Some key topographic and material controls on debris flows in Scotland. *Quarterly Journal of Engineering Geology and Hydrogeology*. 48(3-4):212-223. doi:10.1144/qjegh2013-095.

Mitchell A, McDougall S, Nolde N, Brideau MA, Whittall J, Aaron JB. 2019. Rock avalanche runout prediction using stochastic analysis of a regional dataset. *Landslides*. doi:10.1007/s10346-019-01331-3.

New Zealand Government. 2004. Building Act. Wellington (NZ): Government Printer. Reprint as at 24 October 2019.

New Zealand Government. 1993. Earthquake Commission Act. Wellington (NZ): Government Printer. Reprint as at 1 July 2019.

Reid ME, Brien DL, LaHusen RG, Roering JJ, de la Fuente J, Ellen SD. 2003. Debris-flow initiation from large, slow moving landslides. In: Rickenmann D, Chen CL, editors. *Debris-flow hazards mitigation: Mechanics, prediction, and assessment*. Rotterdam (NL): Millpress Science. p. 151-166.

Scheidegger AE. 1973. On the prediction of the reach and velocity of catastrophic landslides. *Rock mechanics*. 5(4):231-236. doi:10.1007/bf01301796.

Skempton AW, Hutchinson J. 1969. Stability of natural slopes and embankment foundations. In: *Proceedings of the International Conference on Soil Mechanics and Foundation Engineering = Comptes Rendus du Congres International de Mecanique des Sols et des Travaux de Fondations*. Mexico. Mexico City (MX): Sociedad Mexicana de Mecanica de Suelos. p. 291-340.

Snelder T, Biggs B, Weatherhead M. 2010. New Zealand river environment classification user guide. Wellington: Ministry for the Environment; [accessed 2020 Jan 09]. https://www.mfe.govt.nz/sites/default/files/environmental-reporting/about-environmental-reporting/classification-systems/rec-user-guide-2010.pdf

Welsh A, Davies T. 2011. Identification of alluvial fans susceptible to debris-flow hazards. *Landslides*. 8:183-194. doi:10.1007/s10346-010-0238-4.

Welsh AJ, 2007. Delineating debris-flow hazards on alluvial fans in the Coromandel and Kaimai regions, New Zealand, using GIS [MSc thesis]. Christchurch (NZ): University of Canterbury. 190 p.

Whittall J. 2019. Runout estimates and risk-informed decision making for bench scale open pit slope failures. *Canadian Geotechnical Journal*. doi:10.1139/cgj-2018-0462.

Wilford D, Sakals M, Innes J, Sidle R, Bergerud WA. 2004. Recognition of debris flow, debris flood and flood hazard through watershed morphometrics. *Landslides*. 1:61-66. doi:10.1007/s10346-003-0002-0.

Wong HN, Ko FWY, Hui THH, 2004. Assessment of landslide risk of natural hillsides in Hong Kong. Hong Kong: Geotechnical Engineering Office. GEO Report No. 191.

Wong HN, Lam KC, Ho KKS. 1998. Diagnostic report on the November 1993 natural terrain landslides on Lantau Island. Hong Kong: Geotechnical Engineering Office. GEO Report No. 69.

www.gns.cri.nz

Principal Location

1 Fairway Drive, Avalon
Lower Hutt 5010
PO Box 30368
Lower Hutt 5040
New Zealand
T +64-4-570 1444
F +64-4-570 4600

Other Locations

Dunedin Research Centre
764 Cumberland Street
Private Bag 1930
Dunedin 9054
New Zealand
T +64-3-477 4050
F +64-3-477 5232

Wairakei Research Centre
114 Karetoto Road
Private Bag 2000
Taupo 3352
New Zealand
T +64-7-374 8211
F +64-7-374 8199

National Isotope Centre
30 Gracefield Road
PO Box 30368
Lower Hutt 5040
New Zealand
T +64-4-570 1444
F +64-4-570 4657